Sensitivity analysis via Karhunen-Loève expansion of a random field model: estimation of Sobol' indices and experimental design

Luc Pronzato

Sensitivity analysis via Karhunen-Loève expansion of a random field model: estimation of Sobol' indices and experimental design

Luc Pronzato*†

June 22, 2017

Abstract

We use the Karhunen-Loève expansion of a random-field model to construct a tensorised Bayesian linear model from which Sobol' sensitivity indices can be estimated straightforwardly. The method combines the advantages of models built from families of orthonormal functions, which facilitate computations, and Gaussian-process models, which offer a lot of flexibility. The posterior distribution of the indices can be derived, and its normal approximation can be used to design experiments especially adapted to their estimation. Implementation details are provided, and values of tuning parameters are indicated that yield precise estimation from a small number of function evaluations. Several illustrative examples are included that show the good performance of the method, in particular in comparison with estimation based on polynomial chaos expansion.

Keywords: sensitivity analysis, Sobol' indices, random-field model, Karhunen-Loève expansion, Bayesian linear model, polynomial chaos, optimal design of experiments.

1 Introduction and problem statement

We consider global sensitivity analysis for a function $\mathfrak{f}(\cdot)$ depending on d independent real input variables $x_1, \ldots, x_d$, x_i being distributed with the probability measure μ_i over $\mathscr{X}_i \subseteq \mathbb{R}$ for each $i = 1, \ldots, d$, so that the probability measure μ of $\mathbf{x} = (x_1, \ldots, x_d)$ has the tensor-product form

$$\mathrm{d}\mu(\mathbf{x}) = \mathrm{d}\mu_1(x_1) \times \cdots \times \mathrm{d}\mu_d(x_d)\,. \tag{1.1}$$

Global sensitivity analysis aims at identifying important variables, and possibly important interactions between groups of variables, in the sense that they are the most influential in the global behaviour of $\mathfrak{f}(\cdot)$ on the support of μ. The calculation of Sobol' indices, which quantify the portion of the variance of $\mathfrak{f}(\mathbf{x})$ explained by each x_i, or combination of different x_i's, see Section 2.1, has become a standard tool in sensitivity analysis for measuring the importance of (groups of) variables.

Commonly used estimation methods of Sobol' indices include the Fourier Amplitude Sensitivity Test (FAST) [5, 30, 6], see also [29]; the model-free pick-and-freeze methods [31, 28] based on QMC sampling designs, Latin hypercubes (Lh) or orthogonal arrays, see in particular [19, 34, 12, 13]. In case of functions $\mathfrak{f}(\cdot)$ of computationally expensive evaluation, the use of metamodels allows estimation of indices from a reduced number of data points; see e.g., [22, 20]. See also [17] which combines Gaussian-process metamodeling and Monte Carlo sampling. The calculation of Sobol'

*Luc.Pronzato@cnrs.fr (corresponding author)
†Université Côte d'Azur, CNRS, I3S, France

indices is then considerably facilitated when the metamodel used has a particular form, which is especially adapted to the underlying Sobol'-Hoeffding decomposition.

(*i*) Polynomial Chaos Expansions (PCE) correspond to tensor products of univariate polynomial models $P_i(x_i)$, each $P_i(\cdot)$ belonging to a family of orthogonal polynomials with respect to μ_i, and provide an easy evaluation of Sobol' indices. Indeed, the indices are given by ratios of quadratic forms in estimated parameters in the linear regression model defined by the PCE; see [33, 2, 1]. The precision of the estimated indices can be related to the information matrix for the linear regression model, which allows the construction of efficient designs adapted to the estimation of Sobol' indices; see [4]. Families of orthogonal polynomials are known for particular distributions (e.g., Hermite for the standard normal, Legendre for the uniform distribution, etc.), but transformations or calculation via moment matrices can be used in more general situations, see Section 4.1.

(*ii*) To a given Random Field (RF) model with tensor-product covariance (see [32, p. 54]) and a tensorised probability measure μ, one can associate a particular ANOVA kernel that yields a simple expression for the Sobol' indices, see [7]. The construction of the ANOVA kernel is explicit for some particular RF covariances and measures μ only, but numerical integration can be used otherwise. See also [14] for the ANOVA decomposition of a kernel, with some insights into the consequence of enforcing sparsity through the choice of a sparse kernel.

On the other hand, both approaches suffer from some limitations. The number of monomials to be considered in a PCE model grows very fast with the number d of variables, so that many observations (function evaluations) are required to get an estimate of the indices, even for moderate values of d. Moreover, the polynomial model seems to offer less flexibility than a RF model with covariance chosen in a suitable family (for instance the Matérn class, see [32, Chap. 2]) that specifies the regularity of the RF realisations (i.e., of the function to be approximated). In the approach based on ANOVA kernels, no simple characterisation of the precision of the estimation, which could be used for experimental design, is available. Moreover, no simple recursive calculation of the indices seems possible in the case where data are collected successively.

The objective of the paper is to present a method that combines the positive aspects of (*i*) and (*ii*): starting with an arbitrary Gaussian RF model with covariance in the tensor product form, following the approach in [11], we construct a Bayesian Linear Model (BLM) through a particular Karhunen-Loève expansion of the field associated with the tensor-product measure μ; see also [8]. Like in a PCE model, the regression functions of variable i are orthogonal for μ_i, $i = 1, \ldots, d$ (they may possibly also include a few polynomial terms), but in addition to a PCE model the parameters have here a joint prior normal distribution, with known diagonal covariance. The Sobol' indices (*of any order*) are obtained straightforwardly from the estimated parameters in the BLM, and the presence of a prior allows estimation from a few observations only. Like in [4], the linearity of the model facilitates the recursive estimation of the indices in case of sequential data collection. The sequential selection of observation points (sequential design) ensuring a precise estimation of the indices can easily be implemented, and various selection rules can be considered depending on which characterisation of precision is preferred. Approximate design theory can also be used to construct an optimal design measure for the estimation of Sobol' indices through the solution of a convex problem, from which an exact design (without repetitions of observations) can be extracted.

The computation of Sobol' indices via the Karhunen-Loève expansion of a covariance operator is also considered in [9], but in a different framework. The authors consider an additive model with functional inputs and, using properties of U-statistics, they investigate the asymptotic properties of an estimator of first-order indices when the truncation level M of the expansion grows at suitable rate as a function of the number n of observations. The situation is much different in the present paper: we consider a general nonlinear function $\mathfrak{f}(\cdot)$ of scalar inputs and our Karhunen-Loève expansion concerns a random-field model of $\mathfrak{f}(\cdot)$. The number M of regression functions in the obtained BLM

and the regression functions themselves are fixed, with M of the same order of magnitude as the number n of observations to be performed. We shall not investigate the asymptotic properties of our estimator of Sobol' indices as M and n tend to infinity. For fixed M, i.e., for a fixed BLM, the estimated indices tend to the true indices of that BLM as n tends to infinity and satisfy a central limit theorem (under standard assumptions concerning Bayesian estimation in a linear regression model). However, since M is fixed, the estimated indices do not converge to the true indices of $\mathfrak{f}(\cdot)$ as n tends to infinity. Note that we are mainly interested in the case where n is small, a prerequisite when $\mathfrak{f}(\cdot)$ expensive to evaluate, and we are more concerned with the choice of the n design points ensuring a precise estimation of the indices than with asymptotic properties for large n, when $M = M(n)$ grows with n at suitable rate.

The paper is rather long, but several sections which are important for implementing the method can be skipped on a first reading. Section 2 gives a brief overview of the Sobol'-Hoeffding decomposition and the estimation of Sobol'indices in models given by tensor-products of orthonormal functions. The tensorised BLM is introduced in Section 3 for a general measure μ. Its practical implementation relies on finitely supported measures, typically quadrature approximations, and is detailed in Section 4 with some numerical illustrations. Section 5 considers the estimation of Sobol' indices in the BLM, together with the construction of posterior distributions and credible intervals. In Section 6, the normal approximation of the posterior distribution is used to design experiments adapted to the estimation of Sobol' indices. The examples in Section 7 illustrate the performance of the method, in particular in comparison with PCE.

2 Sobol' sensitivity indices

2.1 The Sobol'-Hoeffding decomposition and Sobol' indices

Let $f(\cdot)$ be a function depending on d input variables $\mathbf{x} = (x_1, \ldots, x_d) \in \mathscr{X} \subseteq \mathbb{R}^d$ and μ denote a probability measure on $\mathscr{X}$. We suppose that $f \in L^2(\mathscr{X}, \mu)$, the Hilbert space of real-valued functions on $\mathscr{X}$ square integrable for μ, and that μ has the product-tensor form (1.1). We shall denote by $\mathsf{E}_\mu\{\cdot\}$ and $\mathsf{var}_\mu\{\cdot\}$ the expectation and variance for μ, respectively. Then $f(\cdot)$ admits the following Sobol'-Hoeffding decomposition of $f(\cdot)$ in 2^d terms [31],

$$f(\mathbf{x}) = f_0 + \sum_{i=1}^{d} f_i(x_i) + \sum_{i \le j \le d} f_{i,j}(x_i, x_j) + \sum_{i \le j \le k \le d} f_{i,j,k}(x_i, x_j, x_k) + \cdots + f_{1,\ldots,d}(x_1, \ldots, x_d)\,. \quad (2.1)$$

For $\mathscr{U}$ an index set, $\mathscr{U} \subset \{1, \ldots, d\}$, denote by $f_{\mathscr{U}}(\mathbf{x}_{\mathscr{U}})$ the corresponding term in the decomposition above (without further indication, we shall only consider ordered index sets). For a fixed f_0, when we impose that

$$\forall i \in \mathscr{U}\,, \quad \int_{\mathscr{X}} f_{\mathscr{U}}(\mathbf{x}_{\mathscr{U}})\, \mathrm{d}\mu_i(x_i) = 0\,, \quad (2.2)$$

then the decomposition (2.1) is unique. Moreover, we have the orthogonality property

$$\forall \mathscr{U} \neq \mathscr{V}\,,\ \mathscr{U}, \mathscr{V} \subset \{1, \ldots, d\}\,, \quad \mathsf{E}_\mu\{f_{\mathscr{U}}(\mathbf{X}_{\mathscr{U}}) f_{\mathscr{V}}(\mathbf{X}_{\mathscr{V}})\} = 0\,,$$

together with $f_0 = \mathsf{E}_\mu\{f(\mathbf{X})\}$. The orthogonality property implies that we can decompose the variance of $f(\mathbf{X})$ as

$$\begin{aligned} V = \mathsf{var}_\mu\{f(\mathbf{X})\} &= \sum_{i=1}^{d} \mathsf{var}_\mu\{f_i(X_i)\} + \sum_{i\le j\le d} \mathsf{var}_\mu\{f_{i,j}(X_i,X_j)\} + \cdots + \mathsf{var}_\mu\{f_{1,\ldots,d}(X_1,\ldots,X_d)\} \\ &= \sum_{\mathscr{U}\subset\{1,\ldots,d\}} V_{\mathscr{U}}\,, \end{aligned}$$

where we have denoted $V_{\mathscr{U}} = \mathsf{var}_\mu\{f_{\mathscr{U}}(\mathbf{X}_{\mathscr{U}})\}$. For any $\mathscr{U} \subset \{1,\ldots,d\}$, (2.2) implies that

$$\mathsf{E}_\mu\{f(\mathbf{X})|\mathbf{X}_{\mathscr{U}}) = f_0 + \sum_{\mathscr{V}\subseteq\mathscr{U}} f_{\mathscr{V}}(\mathbf{X}_{\mathscr{V}})\,,$$

so that $V_{\mathscr{U}} = \mathsf{var}_\mu\{\mathsf{E}_\mu\{f(\mathbf{X})|\mathbf{X}_{\mathscr{U}})\} - \sum_{\mathscr{V}\subset\mathscr{U}} V_{\mathscr{V}}$, where the inclusion is strict on the right-hand side. The Sobol' sensitivity index associated with the index set $\mathscr{U}$ is defined by

$$S_{\mathscr{U}} = \frac{V_{\mathscr{U}}}{V}\,.$$

Notice that $\sum_{\mathscr{U}\subset\{1,\ldots,d\}} S_{\mathscr{U}} = 1$. The d first-order indices S_i (respectively, $d(d-1)/2$ second-order indices $S_{i,j}$) correspond to $\mathscr{U} = \{i\}$, $i = 1,\ldots,d$ (respectively, $\mathscr{U} = \{i,j\}$, $(i,j) \in \{1,\ldots,d\}^2$, $i < j$). The closed index associated with $\mathscr{U}$ is defined by

$$\underline{S}_{\mathscr{U}} = \frac{\mathsf{var}_\mu\{\mathsf{E}_\mu\{f(\mathbf{X})|\mathbf{X}_{\mathscr{U}})\}}{V} = \sum_{\mathscr{V}\subseteq\mathscr{U}} S_{\mathscr{V}}\,. \tag{2.3}$$

Also of interest are the so-called total-effect indices,

$$\overline{S}_{\mathscr{U}} = \sum_{\mathscr{V}\cap\mathscr{U}\neq\emptyset} S_{\mathscr{V}} = 1 - \sum_{\mathscr{V}\cap\mathscr{U}=\emptyset} S_{\mathscr{V}} = 1 - \frac{\mathsf{var}_\mu\{\mathsf{E}_\mu\{f(\mathbf{X})|\mathbf{X}_{\{1,\ldots,d\}\setminus\mathscr{U}}\}\}}{V} = \frac{\mathsf{E}_\mu\{\mathsf{var}_\mu\{f(\mathbf{X})|\mathbf{X}_{\{1,\ldots,d\}\setminus\mathscr{U}}\}\}}{V}\,,$$

in particular the d first-order total-effect indices $\overline{S}_i = \overline{S}_{\{i\}}$, $i = 1,\ldots,d$. A group of variables $x_{\mathscr{U}}$ such that $\overline{S}_{\mathscr{U}} \approx 0$ can be considered are having negligible effect on the global behaviour of $f(\cdot)$, which thus allows dimension reduction.

2.2 Sobol' indices for tensor-products of linear combinations of μ_i-orthonormal functions

For all $i = 1,\ldots,d$, let $\{\phi_{i,\ell}(\cdot)\,,\ \ell = 0,\ldots,p_i\}$ denote a collection of $p_i + 1$ orthornormal functions for μ_i; that is, such that

$$\int_{\mathscr{X}_i} \phi_{i,\ell}(x)\,\mathrm{d}\mu_i(x) = 1 \text{ for all } \ell \text{ and } \int_{\mathscr{X}_i} \phi_{i,\ell}(x)\phi_{j,\ell'}(x)\,\mathrm{d}\mu_i(x) = 0 \text{ for all } \ell' \neq \ell\,. \tag{2.4}$$

We suppose moreover that $\phi_{i,0}(x) \equiv 1$ for all i. Consider the tensor-product function defined by

$$f(\mathbf{x}) = \prod_{i=1}^{d} \left[\sum_{\ell=0}^{p_i} \alpha_{i,\ell}\phi_{i,\ell}(x)\right]\,. \tag{2.5}$$

It can be rewritten in the form of a linear regression model having $\prod_{i=1}^d (p_i+1)$ parameters $\beta_{\underline{\ell}}$,

$$f(\mathbf{x}) = \sum_{\underline{\ell}} \beta_{\underline{\ell}} \psi_{\underline{\ell}}(\mathbf{x}) \,,$$

where $\underline{\ell} = \{\ell_1, \ldots, \ell_d\}$ denotes a multi index, with $\ell_i \in \{0, \ldots, p_i\}$ for all $i = 1, \ldots, d$, and where $\beta_{\underline{\ell}} = \prod_{i=1}^d \alpha_{i,\ell_i}$ and $\psi_{\underline{\ell}}(\mathbf{x}) = \prod_{i=1}^d \phi_{i,\ell_i}(x_i)$.

For any index set $\mathscr{U} \subset \{1, \ldots, d\}$, since $\mathsf{E}_{\mu_i}\{\phi_{i,\ell}(X_i)\} = 0$ for all i and all $\ell \neq 0$, we have

$$\mathsf{E}_{\mu}\{f(\mathbf{X})|\mathbf{X}_{\mathscr{U}})\} = \beta_{\underline{0}} + \sum_{\underline{\ell} \in \mathbb{L}(\mathscr{U})} \beta_{\underline{\ell}} \psi_{\underline{\ell}}(\mathbf{X}) \,,$$

where $\underline{0} = \{0, \ldots, 0\}$ and $\mathbb{L}(\mathscr{U}) = \{\underline{\ell} \neq \underline{0} : \ell_i = 0 \text{ for all } i \notin \mathscr{U}\}$. Next, the orthonormality property (2.4) gives

$$\underline{S}_{\mathscr{U}} = \frac{\sum_{\underline{\ell} \in \mathbb{L}(\mathscr{U})} \beta_{\underline{\ell}}^2}{\sum_{\underline{\ell} \neq \underline{0}} \beta_{\underline{\ell}}^2} \,,$$

from which we can easily compute $S_{\mathscr{V}}$ and $\overline{S}_{\mathscr{V}}$ for any index set $\mathscr{V}$, see Section 2.1. In particular,

$$S_i = \underline{S}_{\{i\}} \text{ and } \overline{S}_i = \frac{\sum_{\underline{\ell}:\ell_i \neq 0} \beta_{\underline{\ell}}^2}{\sum_{\underline{\ell} \neq \underline{0}} \beta_{\underline{\ell}}^2} \text{ for all } i = 1 \ldots, d\,, \; S_{i,j} = \underline{S}_{\{i,j\}} - S_i - S_j \text{ for all } i, j = 1 \ldots, d\,.$$

When the $\phi_{i,\ell}(\cdot)$ in (2.5) are univariate polynomials $P_{i,\ell}(\cdot)$ of degree ℓ in a family of orthonormal polynomials for μ_i, the construction of Section 2.2 corresponds to the PCE approach in [33, 2, 1, 4].

3 A tensorised Bayesian linear model

The objective is to construct a linear approximation model for $\mathfrak{f}(\cdot)$, with orthonormal regression functions that satisfy the properties of Section 2.2, together with a prior on the parameters to allow estimation from less observations than parameters. The construction relies on Gaussian RF models with parametric trend given by orthonormal polynomials. In absence of reliable prior information on the behaviour of $\mathfrak{f}(\cdot)$, we recommend to simply replace that trend by a constant term; see Section 4.5. However, the presentation covers the general situation, so that the approach can be considered as an extension of the PCE method of [33, 2]. In this section we consider a theoretical construction which requires the computation of integrals for the measures μ_i. The practical implementation of the model relies on quadrature approximations for the μ_i and will be detailed in Section 4.

3.1 Construction of univariate models

We use the univariate orthonormal polynomials of the PCE model as trend functions for a univariate RF model; that is, for each $i = 1, \ldots, d$ we consider

$$Y_{i,x} = \eta_i(x) + Z_{i,x} \,, \tag{3.1}$$

where $\eta_i(x) = \sum_{\ell=0}^{p_i} \alpha_{i,\ell} P_{i,\ell}(x)$ and where $(Z_{i,x})_{x \in \mathscr{X}_i}$ denotes a Gaussian RF indexed by $\mathscr{X}_i$, with zero mean ($\mathbb{E}\{Z_{i,x}\} = 0$ for all x) and covariance $\mathbb{E}\{Z_{i,x} Z_{i,x'}\} = K_i(x, x')$ for $x, x' \in \mathscr{X}_i$. We denote by $\mathcal{H}_i$ the Reproducing Kernel Hilbert Space (RKHS) of real valued functions on $\mathscr{X}_i$ defined by the kernel $K_i(\cdot, \cdot)$. We suppose that each $K_i(\cdot, \cdot)$ is μ_i-measurable on $\mathscr{X}_i \times \mathscr{X}_i$ and that $\mathsf{E}_{\mu_i}\{K_i(X, X)\} <$

∞. We also suppose that the realisations of $(Z_{i,x})_{x\in\mathscr{X}_i}$ belong to $L^2(\mathscr{X}_i,\mu_i)$ with probability one; see [10, 11] for more precisions. We then consider the following linear operator on $L^2(\mathscr{X}_i,\mu_i)$:

$$\forall f\in L^2(\mathscr{X}_i,\mu_i),\quad \forall t\in\mathscr{X}_i,\quad T_{i,\mu_i}[f](t)=\int_{\mathscr{X}_i} f(x)K_i(t,x)\,\mathrm{d}\mu_i(x)=\mathsf{E}_{\mu_i}\{f(X)K_i(t,X)\}\,.$$

The operator T_{i,μ_i} is compact, positive semidefinite and self-adjoint, and $T_{i,\mu_i}[f]\in\mathcal{H}_{i,\mu_i}$ for all $f\in L^2(\mathscr{X}_i,\mu_i)$, with $\mathcal{H}_{i,\mu_i}$ the closed linear subspace of $\mathcal{H}_i$ orthogonal to $\mathcal{H}_{i,0}=\{h_0\in\mathcal{H}_i : \|h_0\|^2_{L^2(\mathscr{X}_i,\mu_i)}=0\}$.

3.2 Univariate orthogonalisation and kernel reduction

Following [11, Sect. 5.4], for each $i=1,\ldots,d$, we consider the orthogonal projection $\mathfrak{p}_i$ of $L^2(\mathscr{X}_i,\mu_i)$ onto the linear subspace $\mathcal{T}_i$ spanned by the $P_{i,\ell}(\cdot)$, $\ell=0,\ldots,p_i$ and denote $\mathfrak{q}_i=\mathrm{id}_{L^2}-\mathfrak{p}_i$. In matrix notation, denote $\mathbf{g}_i(x)=(P_{i,0}(x),\ldots,P_{i,p_i}(x))^T$ and $\boldsymbol{\alpha}_i=(\alpha_{i,0},\ldots,\alpha_{i,p_i})^T$. From the orthonormality of the $P_{i,\ell}(\cdot)$, we can write, for $x\in\mathscr{X}_i$,

$$\mathfrak{p}_i Z_{i,x}=\mathbf{g}_i^T(x)\mathsf{E}_{\mu_i}\{\mathbf{g}_i(X)Z_{i,X}\}\,, \tag{3.2}$$

with $\mathbb{E}\{\mathfrak{p}_i Z_{i,x}\}=0$ and, for $y\in\mathscr{X}_i$, $\mathbb{E}\{(\mathfrak{p}_i Z_{i,x})(\mathfrak{p}_i Z_{i,y})\}=\mathbf{g}_i^T(x)\mathsf{E}_{\mu_i}\{T_{i,\mu_i}[\mathbf{g}_i](X)\mathbf{g}_i^T(X)\}\mathbf{g}_i(x)$ and $\mathbb{E}\{(\mathfrak{p}_i Z_{i,x})Z_{i,y}\}=\mathbf{g}_i^T(x)T_{i,\mu_i}[\mathbf{g}_i](y)$.

Now, the model (3.1) can be written as

$$Y_{i,x}=\mathbf{g}_i^T(x)\boldsymbol{\alpha}_i+\mathfrak{p}_i Z_{i,x}+\mathfrak{q}_i Z_{i,x}=\mathbf{g}_i^T(x)\boldsymbol{\alpha}_i^{\mathfrak{q}_i}+\mathfrak{q}_i Z_{i,x}, \tag{3.3}$$

with $\boldsymbol{\alpha}_i^{\mathfrak{q}_i}=\boldsymbol{\alpha}_i+\mathsf{E}_{\mu_i}\{\mathbf{g}_i(X)Z_{i,X}\}$. The covariance kernel of $(\mathfrak{q}_i Z_{i,x})_{x\in\mathscr{X}_i}$ in (3.3), called a reduction of the kernel $K_i(\cdot,\cdot)$, is equal to

$$\begin{aligned}K_i^{\mathfrak{q}_i}(x,y) &= \mathbb{E}\{(\mathfrak{q}_i Z_{i,x})(\mathfrak{q}_i Z_{i,y})\}\\ &= K_i(x,y)+\mathbf{g}_i^T(x)\mathsf{E}_{\mu_i}\{T_{i,\mu_i}[\mathbf{g}_i](X)\mathbf{g}_i^T(X)\}\mathbf{g}_i(y)-T_{i,\mu_i}[\mathbf{g}_i^T](x)\mathbf{g}_i(y)-\mathbf{g}_i^T(x)T_{i,\mu_i}[\mathbf{g}_i](y)\,.\end{aligned}$$

Note that in (3.3) we have orthogonality in $L^2(\mathscr{X}_i,\mu_i)$ between the realisations of $(\mathfrak{q}_i Z_{i,x})_{x\in\mathscr{X}_i}$ and the trend subspace $\mathcal{T}_i$, with $\mathfrak{p}_i Z_{i,x}\in\mathcal{T}_i$.

Consider now the integral operator associated with $K_i^{\mathfrak{q}_i}(\cdot,\cdot)$,

$$\forall f\in L^2(\mathscr{X}_i,\mu_i),\quad \forall t\in\mathscr{X}_i,\quad T_{i,\mu_i}^{\mathfrak{q}_i}[f](t)=\mathsf{E}_{\mu_i}\{f(X)K_i^{\mathfrak{q}_i}(t,X)\}\,.$$

By construction, it satisfies $T_{i,\mu_i}^{\mathfrak{q}_i}[P_{i,\ell}]=0$ for all $\ell\in\{0,\cdots,p_i\}$. Like T_{i,μ_i}, it is compact, positive semidefinite and self-adjoint. The set of its strictly positive eigenvalues is at most countable; we shall denote by $\gamma_{i,1}\geq\gamma_{i,2}\geq\cdots$ these eigenvalues ordered by decreasing values and by $\varphi_{i,k}\in L^2(\mathscr{X}_i,\mu_i)$ the associated eigenfunctions, satisfying

$$\forall k\geq 1,\quad T_{i,\mu_i}^{\mathfrak{q}_i}[\varphi_{i,k}]=\gamma_{i,k}\varphi_{i,k}\,,\ \gamma_{i,k}>0\,,$$

and chosen to be orthonormal in $L^2(\mathscr{X}_i,\mu_i)$. We shall also consider their canonical extensions $\varphi'_{i,k}\in\mathcal{H}_i$,

$$\forall x\in\mathscr{X}_i,\quad \varphi'_{i,k}(x)=\frac{1}{\gamma_{i,k}}T_{i,\mu_i}^{\mathfrak{q}_i}[\varphi_{i,k}](x)\,,\ k\geq 1\,, \tag{3.4}$$

so that $\{\sqrt{\gamma_{i,k}}\varphi'_{i,k} : k \geq 1\}$ forms an orthonormal basis of $\mathcal{H}_{i,\mu_i}$ for the Hilbert structure of $\mathcal{H}_i$, see [10, Prop. 3.1]. Notice that the $\varphi'_{i,k}(\cdot)$ are defined over the whole $\mathscr{X}_i$, with $\varphi'_{i,k} = \varphi_{i,k}$ μ_i-almost everywhere, and that $\mathsf{E}_{\mu_i}\{\varphi'_{i,k}(X)P_{i,\ell}(X)\} = 0$ for all $\ell = 1, \ldots, p_i$ and all $l \geq 1$. Also,

$$\sum_{k\geq 1} \gamma_{i,k} = \mathsf{E}_{\mu_i}\{K_i^{\mathfrak{q}_i}(X,X)\} \leq \mathsf{E}_{\mu_i}\{K_i(X,X)\}\,, \tag{3.5}$$

see [11]. Next, we consider the Karhunen-Loève expansion of $\mathfrak{q}_i Z_{i,x}$ in (3.3),

$$\forall x \in \mathscr{X}_i\,, \quad \mathfrak{q}_i Z_{i,x} = \sum_{k\geq 1} \alpha'_{i,k}\varphi'_{i,k}(x) + \varepsilon_{i,0,x}\,,$$

where the $\alpha'_{i,k}$, $k \geq 1$, are mutually orthogonal normal random variables $\mathscr{N}(0, \gamma_{i,k})$ and where $\varepsilon_{i,0,x}$ is a centred RF that belongs to the Gaussian Hilbert space isometric to $\mathcal{H}_{i,0}$ and has covariance $K_i^{\mathfrak{q}_i}(x,y) - \sum_{k\geq 1}\gamma_{i,k}\varphi'_{i,k}(x)\varphi'_{i,k}(y)$. Also, for all $x \in \mathscr{X}_i$, the $\alpha'_{i,k}$ are orthogonal to $\varepsilon_{i,0,x}$. We can thus rewrite (3.3) as

$$Y_{i,x} = \sum_{\ell=0}^{p_i} \alpha_{i,\ell}^{\mathfrak{q}_i} P_{i,\ell}(x) + \sum_{k\geq 1} \alpha'_{i,k}\varphi'_{i,k}(x) + \varepsilon_{i,0,x}\,. \tag{3.6}$$

3.3 Tensorised BLM

We set a prior on the $\alpha_{i,\ell}^{\mathfrak{q}_i}$, and suppose that $\boldsymbol{\alpha}_i^{\mathfrak{q}_i} = (\alpha_{i,0}^{\mathfrak{q}_i}, \ldots, \alpha_{i,p_i}^{\mathfrak{q}_i})^T$ is normally distributed $\mathscr{N}(\mathbf{0}, \mathbf{D}_i)$, with $\mathbf{D}_i = \mathrm{diag}\{\vartheta_{i,\ell},\, \ell = 0, \ldots, p_i\}$, for all $i = 1, \ldots, d$. The choice of the $\vartheta_{i,\ell}$ is discussed in Section 4.3. We then consider the kernels

$$K'_i(x,y) = K_i^{\mathfrak{q}_i}(x,y) + \sum_{\ell=0}^{p_i} \vartheta_{i,\ell} P_{i,\ell}(x)P_{i,\ell}(y)\,, \tag{3.7}$$

and denote the associated RKHS by $\mathcal{H}'_i$. This yields the following tensorised version of model (3.6),

$$Y_{\mathbf{x}} = \sum_{\underline{\ell}\in\mathbb{N}^d} \beta_{\underline{\ell}}\psi_{\underline{\ell}}(\mathbf{x}) + \varepsilon_{0,\mathbf{x}} \tag{3.8}$$

where $\underline{\ell} = \{\ell_1, \ldots, \ell_d\}$ with $\ell_i \in \mathbb{N}$ for all i, and where the $\beta_{\underline{\ell}}$ are independent random variables $\mathscr{N}(0, \Lambda_{\underline{\ell}})$ with $\Lambda_{\underline{\ell}} = \prod_{i=1}^d \lambda_{i,\ell_i}$, $\psi_{\underline{\ell}}(\mathbf{x}) = \prod_{i=1}^d \phi_{i,\ell_i}(x_i)$ for any $\mathbf{x} \in \mathscr{X}$, and

$$\phi_{i,\ell}(\cdot) = \begin{cases} P_{i,\ell}(\cdot) & \text{for } \ell = 0, \ldots, p_i\,, \\ \varphi'_{i,\ell-p_i}(\cdot) & \text{for } \ell \geq p_i + 1\,, \end{cases} \qquad \lambda_{i,\ell}(\cdot) = \begin{cases} \vartheta_{i,\ell} & \text{for } \ell = 0, \ldots, p_i\,, \\ \gamma_{i,\ell-p_i} & \text{for } \ell \geq p_i + 1\,. \end{cases} \tag{3.9}$$

Here, $\varepsilon_{0,\mathbf{x}}$ is a centred RF that belongs to the Gaussian Hilbert space isometric to $\mathcal{H}_0^{\otimes} = \{h \in \otimes_{i=1}^d \mathcal{H}'_i :\, \|h\|^2_{L^2(\mathscr{X},\mu)} = 0\}$ and has covariance $\mathbb{E}\{\varepsilon_{0,\mathbf{x}}\varepsilon_{0,\mathbf{y}}\} = \prod_{i=1}^d K'_i(x_i,y_i) - \sum_{\underline{\ell}\in\mathbb{N}^d} \Lambda_{\underline{\ell}}\psi_{\underline{\ell}}(\mathbf{x})\psi_{\underline{\ell}}(\mathbf{y})$. When truncating the sum in (3.8) to $\underline{\ell}$ in a given finite subset $\mathbb{L}$ of $\mathbb{N}^d$, we obtain the model $Y_{\mathbf{x}} = \sum_{\underline{\ell}\in\mathbb{L}} \beta_{\underline{\ell}}\psi_{\underline{\ell}}(\mathbf{x}) + \varepsilon_{\mathbf{x}}$, where now $\mathbb{E}\{\varepsilon_{\mathbf{x}}\varepsilon_{\mathbf{y}}\} = \prod_{i=1}^d K'_i(x_i,y_i) - \sum_{\underline{\ell}\in\mathbb{L}} \Lambda_{\underline{\ell}}\psi_{\underline{\ell}}(\mathbf{x})\psi_{\underline{\ell}}(\mathbf{y})$. The choice of $\mathbb{L}$ will be discussed in Section 4.4.

Finally, the BLM we shall use for sensitivity analysis is given by

$$Y_{\mathbf{x}} = \sum_{\underline{\ell}\in\mathbb{L}} \beta_{\underline{\ell}}\psi_{\underline{\ell}}(\mathbf{x}) + \varepsilon'_{\mathbf{x}}\,, \tag{3.10}$$

where we have replaced the errors $\varepsilon_{\mathbf{x}}$ by uncorrelated ones $\varepsilon'_{\mathbf{x}}$, such that $\mathbb{E}\{\varepsilon'_{\mathbf{x}}\varepsilon'_{\mathbf{y}}\} = 0$ for $\mathbf{x} \neq \mathbf{y}$ and

$$\forall \mathbf{x} \in \mathscr{X}\,, \quad s^2(\mathbf{x}) = \mathbb{E}\{(\varepsilon'_{\mathbf{x}})^2\} = \mathbb{E}\{(\varepsilon_{\mathbf{x}})^2\} = \prod_{i=1}^{d} K'_i(x_i, x_i) - \sum_{\underline{\ell} \in \mathbb{L}} \Lambda_{\underline{\ell}} \psi^2_{\underline{\ell}}(\mathbf{x})\,. \tag{3.11}$$

Following the results in Section 2.1, the estimation of the parameters $\beta_{\underline{\ell}}$ in (3.10) from evaluations of $\mathfrak{f}(\cdot)$ at a given set of design points will provide estimates of Sobol' indices; see Section 5.

Remark 3.1. We might also consider estimation of $\beta_{\underline{\ell}}$ in the model with correlated errors $\varepsilon_{\mathbf{x}}$. However, estimation with a n-point design would then require the calculation and manipulation of a $n \times n$ correlation matrix, whereas only its n diagonal terms need to be used for the model (3.10). Moreover, this choice of uncorrelated errors will facilitate the construction of experimental designs adapted to the estimation of Sobol' indices, see Section 6. ◁

4 Practical implementation via quadrature approximation

The $\varphi'_{i,k}(\cdot)$ and associated eigenvalues $\gamma_{i,k}$ in (3.6) are usually unknown, and we need to resort to numerical approximations. A convenient practical implementation consists in replacing the measures μ_i by quadrature approximations

$$\widehat{\mu}_i = \sum_{j=1}^{q_i} w_{i,j} \delta_{x_{i,j}}\,.$$

For all $i = 1, \ldots, d$, denote $\mathbf{W}_i = \mathrm{diag}\{w_{i,j},\, j = 1, \ldots, q_i\}$ and $\mathbf{Q}_i$ (respectively, $\mathbf{Q}_i^{\mathfrak{q}_i}$) the matrix with j,k term $\{\mathbf{Q}_i\}_{j,k} = K_i(x_{i,j}, x_{i,k})$ (respectively, $\{\mathbf{Q}_i^{\mathfrak{q}_i}\}_{j,k} = K_i^{\mathfrak{q}_i}(x_{i,j}, x_{i,k})$) for $j,k = 1, \ldots, q_i$. We shall always assume that $\prod_{i=1}^{d} q_i \gg n$, the projected number of evaluations of $\mathfrak{f}(\cdot)$.

Remark 4.1. Since we are considering unidimensional approximations, q_i does not need to be very large, and $q_i = 100$ seems to be enough in most cases, see Sections 4.6 and 7. On the other hand, the $\widehat{\mu}_i$ may also correspond to empirical measures obtained from historical data, a situation where q_i may naturally take large values. ◁

4.1 Construction of $\mathbf{Q}_i^{\mathfrak{q}_i}$

For each $i = 1, \ldots, d$ we consider the family of polynomials $P_{i,\ell}(\cdot)$, of degrees $l = 0, \ldots, p_i \leq q_i - 1$, orthonormal for the measure $\widehat{\mu}_i$. Direct calculation shows that orthonormality implies (up to an arbitrary sign change)

$$P_{i,0}(x) = 1 \;\text{ and }\; P_{i,\ell}(x) = \frac{\det \begin{pmatrix} 1 & m_{i,1} & \cdots & m_{i,\ell} \\ m_{i,1} & m_{i,2} & \cdots & m_{i,\ell+1} \\ \vdots & \vdots & \ddots & \vdots \\ m_{i,\ell-1} & m_{i,\ell} & \cdots & m_{i,2\ell-1} \\ 1 & x & \cdots & x^{\ell} \end{pmatrix}}{\det^{1/2}(\mathbf{M}_{i,\ell}) \det^{1/2}(\mathbf{M}_{i,\ell-1})} \;\text{ for } l \geq 1\,,$$

where, for any $\ell \in \mathbb{N}$, $\mathbf{M}_{i,\ell}$ is the $(\ell+1) \times (\ell+1)$ moment matrix with j,k term $\{\mathbf{M}_{i,\ell}\}_{j,k} = m_{i,j+k-2}$ and $m_{i,k} = \mathsf{E}_{\widehat{\mu}_i}\{X^k\}$ for all k. Denote by $\mathbf{G}_i$ the $q_i \times (p_i + 1)$ matrix with j,ℓ term $\phi_{i,\ell}(x_{i,j})$. It satisfies $\mathbf{G}_i^T \mathbf{W}_i \mathbf{G}_i = \mathbf{I}_{p_i+1}$ and we have, from the definition of $K_i^{\mathfrak{q}_i}(\cdot,\cdot)$,

$$\mathbf{Q}_i^{\mathfrak{q}_i} = \mathbf{Q}_i + \mathbf{G}_i \mathbf{G}_i^T \mathbf{W}_i \mathbf{Q}_i \mathbf{W}_i \mathbf{G}_i \mathbf{G}_i^T - \mathbf{G}_i \mathbf{G}_i^T \mathbf{W}_i \mathbf{Q}_i - \mathbf{Q}_i \mathbf{W}_i \mathbf{G}_i \mathbf{G}_i^T\,, \tag{4.1}$$

from which we can readily check that $\mathbf{Q}_i^{\mathfrak{q}_i} \mathbf{W}_i \mathbf{G}_i = \mathbf{O}_{q_i,(p_i+1)}$, the $q_i \times (p_i + 1)$ null matrix.

4.2 Calculation of $\psi_{\underline{\ell}}(\mathbf{x})$ and $s^2(\mathbf{x})$

We first diagonalise $\mathbf{W}_i^{1/2}\mathbf{Q}_i^{\mathfrak{q}_i}\mathbf{W}_i^{1/2}$ (for the Euclidean structure of $\mathbb{R}^{q_i}$) and compute a matrix $\widetilde{\mathbf{\Phi}}_i$ of eigenvectors and a diagonal matrix $\mathbf{\Gamma}_i$ of associated eigenvalues (sorted by decreasing values) that satisfy $\mathbf{W}_i^{1/2}\mathbf{Q}_i^{\mathfrak{q}_i}\mathbf{W}_i^{1/2} = \widetilde{\mathbf{\Phi}}_i\mathbf{\Gamma}_i\widetilde{\mathbf{\Phi}}_i^T$, with $\widetilde{\mathbf{\Phi}}_i^T\widetilde{\mathbf{\Phi}}_i = \mathbf{I}_{q_i}$, the $q_i \times q_i$ identity matrix. Denote $\mathbf{\Phi}_i = \mathbf{W}_i^{-1/2}\widetilde{\mathbf{\Phi}}_i$; it satisfies $\mathbf{\Phi}_i^T\mathbf{W}_i\mathbf{\Phi}_i = \mathbf{I}_{q_i}$, $\mathbf{Q}_i^{\mathfrak{q}_i} = \mathbf{\Phi}_i\mathbf{\Gamma}_i\mathbf{\Phi}_i^T$ and $\mathbf{Q}_i^{\mathfrak{q}_i}\mathbf{W}_i\mathbf{\Phi}_i = \mathbf{\Phi}_i\mathbf{\Gamma}_i$, so that $\mathbf{G}_i^T\mathbf{W}_i\mathbf{\Phi}_i = \mathbf{O}_{(p_i+1),q_i}$.

Like in [11], we call *quadrature design* of size n a collection $\mathscr{D}_n = \{\mathbf{x}_1, \ldots, \mathbf{x}_n\}$ of n points of $\mathscr{X}$ such that $\{\mathbf{x}_j\}_i = x_{i,j}$ is included in the support of $\widehat{\mu}_i$ for all $j = 1, \ldots, n$ and $i = 1, \ldots, d$.

Consider first a point $\mathbf{x}_j$ in a quadrature design $\mathscr{D}_n$, with $\{\mathbf{x}_j\}_i = x_{i,j}$ for $i = 1, \ldots, d$. In the BLM model (3.10), $\psi_{\underline{\ell}}(\mathbf{x}_j) = \prod_{i=1}^d \phi_{i,\ell_i}(x_{i,j})$ and the $\beta_{\underline{\ell}}$ are independent normal random variables $\mathscr{N}(0, \Lambda_{\underline{\ell}})$ with $\Lambda_{\underline{\ell}} = \prod_{i=1}^d \lambda_{i,\ell_i}$, where the $\phi_{i,\ell}(x_{i,j})$ and $\lambda_{i,\ell}$ are given by (3.9), with $\varphi'_{i,k}(x_{i,j}) = \{\mathbf{\Phi}_i\}_{j,k}$ and $\gamma_{i,k}$ is the kth diagonal element of $\mathbf{\Gamma}_i$. To compute $s^2(\mathbf{x}_j)$ we need to calculate additionally $\prod_{i=1}^d K'_i(x_{i,j}, x_{i,j})$, see (3.11), with

$$K'_i(x_{i,j}, x_{i,j}) = \{\mathbf{Q}_i^{\mathfrak{q}_i}\}_{j,j} + \sum_{\ell=0}^{p_i} \vartheta_{i,\ell} P_{i,\ell}^2(x_{i,j}) = \sum_{\ell=1}^{q_i} \gamma_{i,\ell}\{\mathbf{\Phi}_i\}_{j,\ell}^2 + \sum_{\ell=0}^{p_i} \vartheta_{i,\ell} P_{i,\ell}^2(x_{i,j})\,,$$

see (3.7).

Consider now any $\mathbf{x} \in \mathscr{X}$; its ith coordinate x_i being not necessarily in the support of $\widehat{\mu}_i$. Using expression (3.4) of canonical extensions, we need to compute

$$\boldsymbol{\phi}'_i(x_i) = \mathbf{\Gamma}_i^{-1}\mathbf{\Phi}_i^T\mathbf{W}_i\mathbf{k}_i^{\mathfrak{q}_i}(x_i)\,,$$

the ℓ component of which gives $\varphi'_{i,\ell}(x_i)$ to be used in $\psi_{\underline{\ell}}(\mathbf{x}_j)$, see (3.9), where

$$\mathbf{k}_i^{\mathfrak{q}_i}(x) = \mathbf{k}_i(x) + \mathbf{G}_i\mathbf{G}_i^T\mathbf{W}_i\mathbf{Q}_i\mathbf{W}_i\mathbf{G}_i\mathbf{g}_i(x) - \mathbf{Q}_i\mathbf{W}_i\mathbf{G}_i\mathbf{g}_i(x) - \mathbf{G}_i\mathbf{G}_i^T\mathbf{W}_i\mathbf{k}_i(x)\,,$$

for all $i = 1, \ldots, d$ and all $x \in \mathscr{X}_i$, with $\mathbf{k}_i(x)$ the q_i-dimensional vector

$$\mathbf{k}_i(x) = [K(x, x_{i,1}), \ldots, K(x, x_{i,q_i})]^T.$$

Since $\mathbf{\Phi}_i^T\mathbf{W}_i\mathbf{G}_i = \mathbf{O}_{q_i,(p_i+1)}$, we obtain

$$\boldsymbol{\phi}'_i(x_i) = \mathbf{\Gamma}_i^{-1}\mathbf{\Phi}_i^T\mathbf{W}_i\mathbf{k}_i(x_i) - \mathbf{\Gamma}_i^{-1}\mathbf{\Phi}_i^T\mathbf{W}_i\mathbf{Q}_i\mathbf{W}_i\mathbf{G}_i\mathbf{g}_i(x_i)\,. \tag{4.2}$$

The computation of $\prod_{i=1}^d K'_i(x_i, x_i)$ in (3.11) relies on

$$K'_i(x, x) = K_i(x, x) + \mathbf{g}_i^T(x)\mathbf{G}_i^T\mathbf{W}_i\mathbf{Q}_i\mathbf{W}_i\mathbf{G}_i\mathbf{g}_i(x) - 2\,\mathbf{g}_i^T(x)\mathbf{G}_i^T\mathbf{W}_i\mathbf{k}_i(x) + \sum_{\ell=0}^{p_i} \vartheta_{i,\ell} P_{i,\ell}^2(x)\,, \tag{4.3}$$

for all $i = 1, \ldots, d$ and all $x \in \mathscr{X}_i$; see (3.7).

Remark 4.2. When $p_i \geq 1$, if $\widehat{\mu}_i$ is a quadrature approximation of μ_i for which orthogonal polynomials $P_{i,\ell}(\cdot)$ are known, we shall simply use $\{\mathbf{G}_i\}_{j,\ell} = P_{i,\ell}(x_i^{(j)})$, although the $P_{i,\ell}(\cdot)$ are not orthonormal for $\widehat{\mu}_i$. However, we must then modify the orthogonal projection (3.2) into

$$\mathfrak{p}_i Z_{i,x} = \mathbf{g}_i^T(x)\mathbf{M}_{\mathbf{g}_i}^{-1}\mathsf{E}_{\mu_i}\{\mathbf{g}_i(X)Z_{i,X}\}\,,$$

with $\mathbf{M}_{\mathbf{g}_i}$ the $p_i \times p_i$ Gram matrix $\mathsf{E}_{\mu_i}\{\mathbf{g}_i(X)\mathbf{g}_i^T(X)\}$. (We suppose that μ_i is such that $\mathbf{M}_{\mathbf{g}_i}$ is invertible.) The expression of $K_i^{\mathfrak{q}_i}(x,y)$ must be modified accordingly, into

$$\begin{aligned} K_i^{\mathfrak{q}_i}(x,y) &= K_i(x,y) + \mathbf{g}_i^T(x)\mathbf{M}_{\mathbf{g}_i}^{-1}\mathsf{E}_{\mu_i}\{T_{i,\mu_i}[\mathbf{g}_i](X)\mathbf{g}_i^T(X)\}\mathbf{M}_{\mathbf{g}_i}^{-1}\mathbf{g}_i(y) \\ &\quad - T_{i,\mu_i}[\mathbf{g}_i^T](x)\mathbf{M}_{\mathbf{g}_i}^{-1}\mathbf{g}_i(y) - \mathbf{g}_i^T(x)\mathbf{M}_{\mathbf{g}_i}^{-1}T_{i,\mu_i}[\mathbf{g}_i](y)\,, \end{aligned}$$

and (4.1) becomes

$$\mathbf{Q}_i^{\mathfrak{q}_i} = \mathbf{Q}_i + \mathbf{G}_i\mathbf{M}_{\mathbf{g}_i}^{-1}\mathbf{G}_i^T\mathbf{W}_i\mathbf{Q}_i\mathbf{W}_i\mathbf{G}_i\mathbf{M}_{\mathbf{g}_i}^{-1}\mathbf{G}_i^T - \mathbf{G}_i\mathbf{M}_{\mathbf{g}_i}^{-1}\mathbf{G}_i^T\mathbf{W}_i\mathbf{Q}_i - \mathbf{Q}_i\mathbf{W}_i\mathbf{G}_i\mathbf{M}_{\mathbf{g}_i}^{-1}\mathbf{G}_i^T\,.$$

Also, when $\mathbf{x}$ is not a quadrature point, (4.2) and (4.3) must be modified into

$$\boldsymbol{\phi}_i'(x_i) = \boldsymbol{\Gamma}_i^{-1}\boldsymbol{\Phi}_i^T\mathbf{W}_i\mathbf{k}_i(x_i) - \boldsymbol{\Gamma}_i^{-1}\boldsymbol{\Phi}_i^T\mathbf{W}_i\mathbf{Q}_i\mathbf{W}_i\mathbf{G}_i\mathbf{M}_{\mathbf{g}_i}^{-1}\mathbf{g}_i(x_i) \tag{4.4}$$

and

$$\begin{aligned} K_i'(x,x) &= K_i(x,x) + \mathbf{g}_i^T(x)\mathbf{M}_{\mathbf{g}_i}^{-1}\mathbf{G}_i^T\mathbf{W}_i\mathbf{Q}_i\mathbf{W}_i\mathbf{G}_i\mathbf{M}_{\mathbf{g}_i}^{-1}\mathbf{g}_i(x) - 2\,\mathbf{g}_i^T(x)\mathbf{M}_{\mathbf{g}_i}^{-1}\mathbf{G}_i^T\mathbf{W}_i\mathbf{k}_i(x) \\ &\quad + \sum_{\ell=0}^{p_i}\vartheta_{i,\ell}P_{i,\ell}^2(x)\,. \end{aligned}$$

◁

Remark 4.3. In some situations, several designs have to be considered, all being subsets of a finite design space $\mathscr{X}_Q = \{\mathbf{x}^{(1)},\dots,\mathbf{x}^{(Q)}\} \subset \mathscr{X}^Q$, for instance $\mathscr{X}_Q$ may be given by the first Q points of a low discrepancy sequence in $\mathscr{X}$. This is the case in particular when selecting a n-point design among $\mathscr{X}_Q$, see Section 6. It is then advantageous to compute all $\boldsymbol{\phi}_i'(\{\mathbf{x}^{(j)}\}_i)$ given by (4.2) and all $K_i'(\{\mathbf{x}^{(j)}\}_i,\{\mathbf{x}^{(j)}\}_i)$ given by (4.3) in advance, for $j = 1,\dots,Q$ and $i = 1,\dots,d$. ◁

4.3 Choice of $\vartheta_{i,\ell}$, $\ell = 0,\dots,p_i$

The selection of eigenfunctions in (3.10) will rely on the energy of each component, measured by the associated eigenvalues, see Section 4.4. It is therefore important to choose values of $\vartheta_{i,\ell}$ for $\ell = 0,\dots,p_i$ large enough to ensure that important polynomial trend functions will be kept in the model, but not too large to allow the preference of eigenfunctions if necessary. There is some arbitrariness in this construction, but we think the suggestion below is suitable in most situations.

We shall use stationary kernels $K_i(\cdot,\cdot)$, so that we can assume (without any loss of generality) that $K_i(x,x) = 1$ for all $x \in \mathscr{X}_i$ and each $i = 1,\dots,d$. Indeed, in (3.10), we can write the variance of $\beta_{\underline{\ell}}$ as $\sigma^2\Lambda_{\underline{\ell}}$ and the variance of $\varepsilon_{\mathbf{x}}'$ as $s^2(\mathbf{x}) = \sigma^2\left[\prod_{i=1}^d K_i'(x_i,x_i) - \sum_{\underline{\ell}\in\mathbb{L}}\Lambda_{\underline{\ell}}\psi_{\underline{\ell}}^2(\mathbf{x})\right]$ for some positive scalar σ^2, and then estimate σ^2 from the data; see Section 5.2. From (3.5), we have $\sum_{k\geq 1}\gamma_{i,k} \leq 1$, and we can take $\vartheta_{i,0} = 1$ for all i. When $p_i \geq 1$, in order to favour the selection of low degree polynomials, we suggest to take $\vartheta_{i,\ell} = \kappa_i^\ell$ with $\kappa_i = \gamma_{i,1}^{1/(1+p_i)}$, so that $\vartheta_{i,\ell} > \gamma_{i,k}$ for all $\ell = 0,\dots,p_i$ and all $k \geq 1$.

4.4 Choice of the truncation set $\mathbb{L}$

In PCE, when considering the tensor product of polynomials up to degree p_i in variable x_i, the model can have up to $\prod_{i=1}^d(1+p_i)$ terms. A rather usual approach consists in favouring simple models by setting a constraint on the total degree D of the polynomial in d variables; the resulting model has then $\binom{d+D}{d}$ parameters (the cardinality of the set $\{\underline{\ell} = \{\ell_1,\dots,\ell_d\} \in \mathbb{N}^d : \sum_{\ell=1}^d \leq D\}$).

Here we suggest to base the selection of terms in (3.10) on the ranking of the eigenvalues $\Lambda_{\underline{\ell}}$. We first choose a number $N \leq \overline{N} = \prod_{i=1}^d(p_i+q_i+1)$ that sets a lower bound on the size of the model

(the number of terms we want to consider) — a value of N of the same order of magnitude as the projected number of evaluations of $\mathfrak{f}(\cdot)$ seems reasonable. Let $\Lambda_{\underline{\ell}_1} \geq \cdots \geq \Lambda_{\underline{\ell}_k} \geq \Lambda_{\underline{\ell}_{k+1}} \geq \cdots$ denote the ordered sequence of the $\Lambda_{\underline{\ell}} = \prod_{i=1}^{d} \lambda_{i,\ell_i}$, with $\underline{\ell} = \{\ell_1, \ldots, \ell_d\} \in \mathbb{N}^d$, where we set $\Lambda_{\{\ell_1,\ldots,\ell_d\}} = 0$ when $\ell_i > p_i + q_i + 1$ for some i. Note that $\underline{\ell}_1 = \underline{0} = \{0, \ldots, 0\}$ and $\Lambda_{\underline{\ell}_1} = 1$; see Section 4.3. Our truncation set is then

$$\mathbb{L}_N = \{\underline{\ell}_1, \ldots, \underline{\ell}_M \in \mathbb{N}^d, \text{ with } M \text{ the smaller integer } \geq N \text{ such that } \Lambda_{\underline{\ell}_M} < \Lambda_{\underline{\ell}_{M+1}}\}\,. \tag{4.5}$$

Remark 4.4. We do not need to compute all the $\overline{N}$ values $\Lambda_{\underline{\ell}_k}$, and the construction of $\mathbb{L}_N$ can be sequential since the $\lambda_{i,k}$ are ordered (by decreasing values) for each i. Also, due to the truncation operated in the construction of $\mathbb{L}_N$, in theory we do not need to compute all q_i eigenpairs in the spectral decomposition of Section 4.2. The resulting computational gain may be marginal when each approximation $\widehat{\mu}_i$ has a small numbers q_i of components, but may be significant when the $\widehat{\mu}_i$ correspond to empirical data; see Remark 4.1. ◁

Remark 4.5. In the special case where all $\widehat{\mu}_i$ are identical and are supported on q points, and $p_i = p$ for all i, all matrices $\mathbf{Q}_i$ are identical, and the same is true for $\mathbf{Q}_i^{\mathfrak{q}_i}$, $\mathbf{\Phi}_i$, $\mathbf{\Gamma}_i$, etc. The model (3.10) has m^d terms at most, with $m = p + q + 1$. Each $\Lambda_{\underline{\ell}}$ can be written as

$$\Lambda_{\underline{\ell}} = \lambda_0^{a_0} \times \cdots \times \lambda_{m-1}^{a_{m-1}}\,, \tag{4.6}$$

with $a_k = \mid \{i : \ell_i = k\} \mid$ and $\sum_{k=0}^{m-1} a_k = d$. The $\Lambda_{\underline{\ell}}$ can thus take $\binom{d+m-1}{m-1}$ different values at most; there are at least $d!/(a_0! \times \cdots a_{m-1}!)$ different $\psi_{\underline{\ell}}(\cdot)$ associated with the same $\Lambda_{\underline{\ell}}$ given by (4.6). ◁

4.5 The special case $p_i = 0$

The construction of the BLM is simpler when $p_i = 0$ (i.e., when the trend $\eta_i(\cdot)$ in (3.1) is a constant, $\eta_i(x) = \alpha_{i,0}$ for all x), for all $i = 1, \ldots, d$. Then, $\mathbf{g}_i(x) = 1$ for all i and x, and the reduced kernel $K_i^{\mathfrak{q}_i}(x, y)$ is given by

$$K_i^{\mathfrak{q}_i}(x, y) = K_i(x, y) + \mathsf{E}_{\mu_i}\{K_i(X, Y)\} - \mathsf{E}_{\mu_i}\{K(x, X)\} - \mathsf{E}_{\mu_i}\{K(y, X)\}\,;$$

(4.1) becomes

$$\mathbf{Q}_i^{\mathfrak{q}_i} = \mathbf{Q}_i + \mathbf{1}_{q_i}(\mathbf{1}_{q_i}^T \mathbf{W}_i \mathbf{Q}_i \mathbf{W}_i \mathbf{1}_{q_i})\mathbf{1}_{q_i}^T - \mathbf{1}_{q_i}\mathbf{1}_{q_i}^T \mathbf{W}_i \mathbf{Q}_i - \mathbf{Q}_i \mathbf{W}_i \mathbf{1}_{q_i}\mathbf{1}_{q_i}^T\,,$$

with $\mathbf{1}_{q_i}$ the q_i-dimensional vector of ones, and (4.2) and (4.3) respectively become

$$\boldsymbol{\phi}_i'(x) = \mathbf{\Gamma}_i^{-1}\mathbf{\Phi}_i^T \mathbf{W}_i \mathbf{k}_i(x) - \mathbf{\Gamma}_i^{-1}\mathbf{\Phi}_i^T \mathbf{W}_i \mathbf{Q}_i \mathbf{W}_i \mathbf{1}_{q_i}$$

and

$$K_i'(x, x) = K_i(x, x) + \mathbf{1}_{q_i}^T \mathbf{W}_i \mathbf{Q}_i \mathbf{W}_i \mathbf{1}_{q_i} - 2\,\mathbf{k}_i(x)^T \mathbf{W}_i \mathbf{1}_{q_i} + \sum_{\ell=0}^{p_i} \vartheta_{i,\ell} P_{i,\ell}^2(x)\,.$$

We only need to choose $\vartheta_{i,0}$ in (3.9), and we can take $\vartheta_{i,0} = 1$ for all i; see Section 4.3.

4.6 Numerical illustrations

Consider the Matérn 3/2 covariance function, given by $K_{3/2}(x, y; \theta) = (1+\sqrt{3}\theta|x-y|)\exp(-\sqrt{3}\theta|x-y|)$; see [32, Chap. 2]. A zero-mean Gaussian process with this covariance is one-time mean-square differentiable. Suppose that μ_1 is the uniform measure on $[0, 1]$, and consider the discrete approximation $\widehat{\mu}_1(q_1)$ that puts weight $1/q_1$ on each of the q_1 points $x_{1,j} = (j-1)/(q_1-1)$, $j = 1, \ldots, q_1$. We

take $p_1 = 2$, and the $P_{1,0}(\cdot)$ in (3.6) are the first three orthonormal polynomials for μ_1: $P_{1,0}(x) = 1$, $P_{1,1}(x) = \sqrt{3}(2x-1)$ and $P_{1,2}(x) = \sqrt{5}(6x^2 - 6x + 1)$.

Figure 1-left shows the values of the components of the first three eigenvectors $\varphi'_{1,\ell}(x_{1,j}) = \{\mathbf{\Phi}_1\}_{j,\ell}$ of the reduced kernel for $j = 1, \ldots, q_1$ and $\ell = 1$ (triangles), $\ell = 2$ (circles) and $\ell = 3$ (crosses), when $q_1 = 20$, $\theta = 2$ (top) and $\theta = 20$ (bottom). Their canonical extensions $\varphi'_{1,\ell}(x)$, $x \in [0,1]$, obtained from (4.4), are plotted in dashed-line. They are orthonormal for $\widehat{\mu}_1(20)$, and close to being orthonormal and orthogonal to the $P_{i,\ell}(x)$ (plotted in full line) for μ_1; see Table 1. The components of the first three eigenvectors obtained when $q_1 = 100$ are indicated by dots. One may notice the good agreement with the canonical extensions $\varphi'_{1,\ell}(x)$ based on 20 points only. We shall use $q_i = 100$ in the examples of Section 7 to ensure quasi-orthonormality of the $\psi_{\underline{\ell}}(\cdot)$ in (3.10), see Table 2.

	$P_{1,0}$	$P_{1,1}$	$P_{1,2}$	$\varphi'_{1,1}$	$\varphi'_{1,2}$	$\varphi'_{1,3}$
$P_{1,0}$	1	0	0	≈ 0	0.0803	≈ 0
$P_{1,1}$	·	1	0	-0.1468	≈ 0	0.1447
$P_{1,2}$	·	·	1	≈ 0	0.1879	≈ 0
$\varphi'_{1,1}$	·	·	·	0.9208	≈ 0	0.1295
$\varphi'_{1,2}$	·	·	·	·	0.9314	≈ 0
$\varphi'_{1,3}$	·	·	·	·	·	0.9247

Table 1: Inner products $\langle \phi_{1,\ell}, \phi_{1,\ell'} \rangle_{L^2(\mathscr{X},\mu)}$ between regression functions used in (3.6) for canonical extensions $\varphi'_{1,j}(\cdot)$ based on a 20-point quadrature approximation with covariance $K_{3/2}(x, y; 2)$ and μ uniform on $[0,1]$ (≈ 0 means an absolute value less than 10^{-15}).

	$P_{1,0}$	$P_{1,1}$	$P_{1,2}$	$\varphi'_{1,1}$	$\varphi'_{1,2}$	$\varphi'_{1,3}$
$P_{1,0}$	1	0	0	≈ 0	-0.0180	≈ 0
$P_{1,1}$	·	1	0	0.0304	≈ 0	0.0322
$P_{1,2}$	·	·	1	≈ 0	-0.0408	≈ 0
$\varphi'_{1,1}$	·	·	·	0.9799	≈ 0	-0.0320
$\varphi'_{1,2}$	·	·	·	·	0.9779	≈ 0
$\varphi'_{1,3}$	·	·	·	·	·	0.9762

Table 2: Inner products $\langle \phi_{1,\ell}, \phi_{1,\ell'} \rangle_{L^2(\mathscr{X},\mu)}$ between regression functions used in (3.6) for canonical extensions $\varphi'_{1,j}(\cdot)$ based on a 100-point quadrature approximation with covariance $K_{3/2}(x, y; 2)$ and μ uniform on $[0,1]$ (≈ 0 means an absolute value less than 10^{-15}).

Figure 1-right shows the values of the $\lambda_{i,\ell}$ in (3.9) for $\ell = 0, \ldots, 10$. The eigenvalues $\gamma_{1,\ell}$ associated with the $\varphi'_{1,\ell}$, see (3.9), are indicated by stars; the values of $\vartheta_{1,\ell} = \gamma_{1,1}^{\ell/(1+p_1)} = \gamma_{1,1}^{\ell/3}$ in (3.9) (see Section 4.3) for $\ell = 0, 1, 2$ are indicated by triangles. We can see that θ (the inverse of the correlation length) has a moderate influence on the first eigenfunctions of the decomposition, but the decrease of eigenvalues is significantly slower for $\theta = 20$ (bottom) than for $\theta = 2$ (top), which has a noticeable impact on the prior distribution of Sobol' indices; see Section 7. The choice of θ should preferably agree with prior information on the fluctuations of $\mathfrak{f}(\cdot)$. In absence of such prior knowledge, a possible guideline is to select a value of θ compatible with the projected number

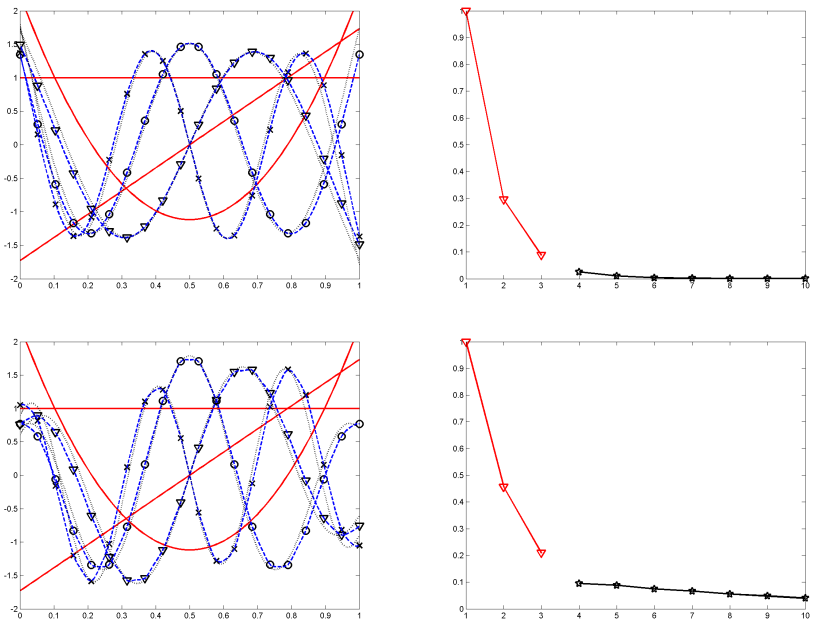

Figure 1: First eigenfunctions (left) and eigenvalues (right) for the univariate model with uniform measure on $[0,1]$ and Matérn covariance $K_{3/2}(\cdot,\cdot;\theta)$, for $\theta = 2$ (top) and $\theta = 20$ (bottom).

n of function evaluations: a model with about n components should be able to capture the global behaviour of $\mathfrak{f}(\cdot)$ over $\mathscr{X}$. A value of θ such that

$$\rho(\theta) = \frac{\sum_{k=1}^{n} \Lambda_{\underline{\ell}_k}}{\sum_{k} \Lambda_{\underline{\ell}_k}} = \frac{\sum_{k=1}^{n} \Lambda_{\underline{\ell}_k}}{\prod_{i=1}^{d} \left(\sum_{\ell=1}^{p_i+q_i+1} \lambda_{i,\ell} \right)} \simeq 1\,, \tag{4.7}$$

see (3.9), thus seems reasonable. For instance, when $n = 64$ and $p_i = 2$ for all i, we obtain here $\rho(2) \simeq 0.9993$ and $\rho(20) \simeq 0.8290$ for $d = 2$, and $\rho(2) \simeq 0.9845$ and $\rho(20) \simeq 0.5083$ for $d = 3$, suggesting that 64 evaluations of a function of three variables may not be enough to reproduce its behaviour with a tensorised model based on Matérn $3/2$ covariance with $\theta = 20$ and second-degree polynomials in each variable. The posterior distributions of the model parameters $\beta_{\underline{\ell}}$ and Sobol' indices depend on θ and rely on strong assumptions on the underlying model; they should thus be taken with caution. As Section 7 will illustrate, they can, however, be used as guidelines for designing experiments adapted to the estimation of Sobol' indices.

Remark 4.6. Another option, which we shall not develop in this paper due to space-limitation, is to estimate θ from the data, by maximum likelihood or cross validation, before the eigendecomposition, using the tensorised covariance kernel $K(\mathbf{x},\mathbf{y};\theta) = \prod_{i=1}^{d} K_i'(x_i,y_i;\theta)$, where the $K_i'(\cdot,\cdot;\theta)$ are given by (3.7). This requires specifying values for the $\vartheta_{i,\ell}$, but does not raise particular difficulties when $p_i = 0$ for all i: one may simply take all $\vartheta_{i,0}$ equal to 1, see Section 4.3. The problem then boils down to estimating covariance parameters θ in a RF model with unknown mean and covariance $\prod_{i=1}^{d}[1 + K_i^{\mathfrak{q}_i}(x_i,y_i;\theta)] - 1$. ◁

The results obtained with the Matérn $5/2$ covariance function, $K_{5/2}(x,y;\theta) = (1+\sqrt{5}\theta|x-y| + 5\theta^2|x-y|^2/3)\exp(-\sqrt{5}\theta|x-y|)$, for the same values of θ as above, yield plots hardly distinguishable

from those presented in Figure 1. Similar experiments with other covariance functions confirm the intuition that the choice of the kernel among a class of smooth enough stationary kernels has little influence when considering only a few terms of the eigendecomposition.

Suppose now that $d = 2$, with $\mu_1 = \mu_2$ uniform on $[0, 1]$, and consider the tensorised model (3.10). We take $p_1 = p_2 = 2$ and use the covariance $K_{3/2}(x, y; 2)$ in each dimension, with the 100-point quadrature approximation $\widehat{\mu}_1(100)$. For $N = 25$, the truncation set $\mathbb{L}_N$ defined by (4.5) is equal to

$$\mathbb{L}_{25} = \left\{ \begin{array}{c} 0\,0\,1\,1\,0\,2\,1\,2\,0\,3\,0\,4\,2\,1\,3\,0\,5\,1\,4\,2\,3\,0\,6\,1\,5 \\ 0\,1\,0\,1\,2\,0\,2\,1\,3\,0\,4\,0\,2\,3\,1\,5\,0\,4\,1\,3\,2\,6\,0\,5\,1 \end{array} \right\}$$

The corresponding values of (log of) $\Lambda_{\underline{\ell}}$ are shown in Figure 2, see (4.6). The construction of the ϑ_{i,ℓ_i} in Section 4.3 implies that $\lambda_{1,\ell}\lambda_{2,\ell'} = \gamma_{1,1}^{(\ell+\ell')/3}$ for $\ell, \ell' \in \{0, \ldots, 3\}$, which explains the presence of a triple and a quadruple of identical $\Lambda_{\underline{\ell}}$; pairs of identical values are simply due to an exchange between dimension indices, i.e., $\lambda_{1,\ell}\lambda_{2,\ell'} = \lambda_{2,\ell}\lambda_{1,\ell'}$.

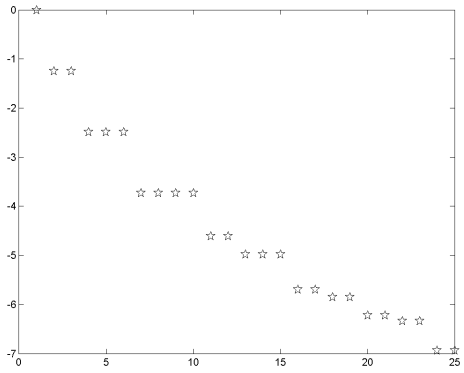

Figure 2: Eigenvalues $\Lambda_{\underline{\ell}}$ (log scale) in the tensorised model.

Besides the 9 polynomial components $P_{1,\ell}(x_1)P_{2,\ell'}(x_2)$, $\ell, \ell' \in \{0, 1, 2\}$, the model (3.10) also contains 16 components that involve (canonical extensions of) eigenfunctions $\varphi'_{i,j}(\cdot)$, for $i = 1, 2$ and $j \in \{1, \ldots, 6\}$. A random realisation of $\sum_{\underline{\ell} \in \mathbb{L}_{25}} \beta_{\underline{\ell}} \psi_{\underline{\ell}}(\mathbf{x})$ in (3.10), with $\beta_{\underline{\ell}}$ independently normally distributed $\mathcal{N}(0, \Lambda_{\underline{\ell}})$, is presented in Figure 3-left. Increasing N in $\mathbb{L}_N$ allows modelling thinner details in the behaviour of $\mathfrak{f}(\cdot)$, as illustrated by Figure 3-right which uses $N = 125$ with the same collection of eigenfunctions. Clearly, a more precise modelling calls for a larger number of observations, this is why we suggest to choose N of the same order of magnitude as the projected number of evaluations of $\mathfrak{f}(\cdot)$.

5 Estimation of Sobol' indices and credible intervals

Suppose that n evaluations of $\mathfrak{f}(\cdot)$ at $\mathscr{D}_n = \{\mathbf{x}_1, \ldots, \mathbf{x}_n\} \subset \mathscr{X}^n$ have been performed, and denote

$$\mathbf{Y}_n = [\mathfrak{f}(\mathbf{x}_1), \ldots, \mathfrak{f}(\mathbf{x}_n)]^T .$$

Also, in the BLM (3.10) with $\mathbb{L} = \mathbb{L}_N$ given by (4.5), denote $\mathbf{\Lambda} = \mathrm{diag}\{\Lambda_{\underline{\ell}_k},\, k = 1, \ldots, M\}$, $\mathbf{\Psi}_n$ the $n \times M$ matrix with j, k term $\psi_{\underline{\ell}_k}(\mathbf{x}_j)$, for $j = 1, \ldots, n$, $k = 1, \ldots, M$, and $\mathbf{\Sigma}_n = \mathrm{diag}\{s^2(\mathbf{x}_j),\, j = 1, \ldots, n\}$ with $\sigma^2(\mathbf{x})$ given by (3.11). The parameters $\boldsymbol{\beta} = (\beta_{\underline{\ell}_1}, \ldots, \beta_{\underline{\ell}_M})^T$ have the normal prior

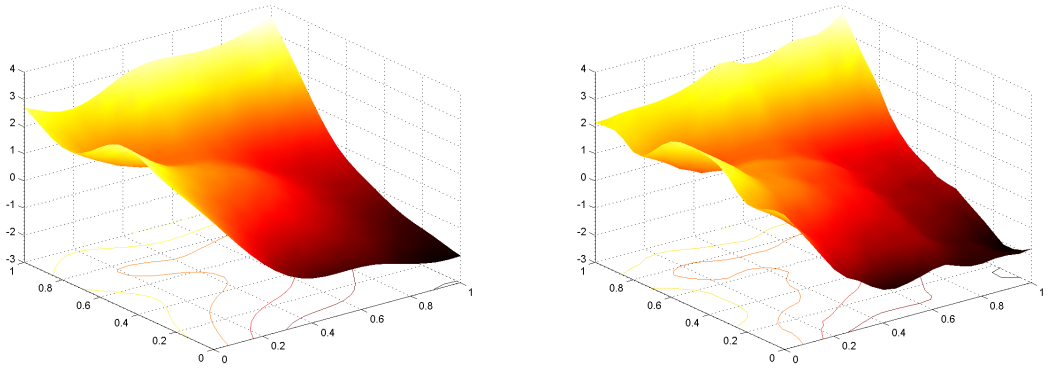

Figure 3: Random realisations of the model response (3.10) for parameters $\beta_{\underline{\ell}}$ having the normal prior $\mathcal{N}(0, \Lambda_{\underline{\ell}})$ and truncation level $N = 25$ (left) and $N = 125$ (right) in (4.5). The tensorisation uses $K_{3/2}(x, y; 2)$ in each dimension with a 100-point quadrature approximation.

$\mathcal{N}(\mathbf{0}, \sigma^2\mathbf{\Lambda})$ and the errors $\boldsymbol{\varepsilon}'_n = [\varepsilon'(\mathbf{x}_1), \ldots, \varepsilon'(\mathbf{x}_n)]$ are normally distributed $\mathcal{N}(\mathbf{0}, \sigma^2\mathbf{\Sigma}_n)$, see Section 4.3. However, the introduction of a prior on the trend parameters in Section 3.3 was only motivated by the construction of the tensorised model, and when estimating $\boldsymbol{\beta}$ we shall put an improper prior on the $\beta_{\underline{\ell}_k}$ that correspond to pure trend components in (3.10); that is, we set $\Lambda_{\underline{\ell}_k}^{-1} = 0$ for all k such that $\ell_{k,i} \leq p_i$ for all $i = 1, \ldots, d$. We denote by $\mathbf{\Lambda}_0$ the corresponding diagonal matrix. We also denote by $\mathbb{K}$ the set of such k, with $|\mathbb{K}| = K$, and $\mathbf{\Lambda}' = \mathrm{diag}\{\Lambda_{\underline{\ell}_k} : k \in \{1, \ldots, M\} \setminus \mathbb{K}\}$; $\mathbf{R}_n$ is the matrix formed by the columns of $\mathbf{\Psi}_n$ with indices in $\mathbb{K}$ and $\mathbf{\Psi}'_n$ is formed by the remaining columns to $\mathbf{\Psi}_n$; $\boldsymbol{\alpha}$ is formed by the K components of $\boldsymbol{\beta}$ with indices in $\mathbb{K}$ and $\boldsymbol{\beta}'$ by the other components of $\boldsymbol{\beta}$, having the prior distribution $\mathcal{N}(\mathbf{0}, \sigma^2\mathbf{\Lambda}')$.

5.1 Estimation of indices

We estimate $\boldsymbol{\beta}$ by its posterior mean

$$\hat{\boldsymbol{\beta}}^n = \mathbf{M}_n^{-1}\mathbf{\Psi}_n^T\mathbf{\Sigma}_n^{-1}\mathbf{Y}_n\,,$$

with $\mathbf{M}_n$ the Bayesian information matrix

$$\mathbf{M}_n = \mathbf{\Psi}_n^T\mathbf{\Sigma}_n^{-1}\mathbf{\Psi}_n + \mathbf{\Lambda}_0^{-1}\,. \tag{5.1}$$

Note that when the data $[\mathbf{x}_k, \mathfrak{f}(\mathbf{x}_k)]$ arrive sequentially, classical recursive least squares formulae can be used to avoid repetitions of matrix inversion. Following the developments in Section 2.2, for any index set $\mathscr{U} \subset \{1, \ldots, d\}$ we estimate $\underline{S}_{\mathscr{U}}$, defined in (2.3), by

$$\widehat{\underline{S}}^n_{\mathscr{U}} = \frac{\sum_{\underline{\ell} \in \mathbb{L}_N(\mathscr{U})} (\hat{\beta}^n_{\underline{\ell}})^2}{\sum_{\underline{\ell} \in \mathbb{L}^*_N} (\hat{\beta}^n_{\underline{\ell}})^2}\,, \tag{5.2}$$

where $\mathbb{L}^*_N = \{\underline{\ell}_k \in \mathbb{L}_N : \underline{\ell}_k \neq \underline{0}\} = \{\underline{\ell}_2, \ldots, \underline{\ell}_M\}$ and $\mathbb{L}_N(\mathscr{U}) = \{\underline{\ell}_k \in \mathbb{L}^*_N : \ell_{k,i} = 0 \text{ for all } i \notin \mathscr{U}\}$, see Section 4.4. This allows us to estimate all Sobol' indices $S_{\mathscr{V}}$ and $\overline{S}_{\mathscr{V}}$ for any index set $\mathscr{V}$, see Section 2. Any such estimate has the form

$$\widehat{S}^n = \frac{\sum_{\underline{\ell}_k \in \tilde{\mathbb{L}}_N} (\hat{\beta}^n_{\underline{\ell}_k})^2}{\sum_{k=2}^{M} (\hat{\beta}^n_{\underline{\ell}_k})^2}\,,$$

for some subset $\widetilde{\mathbb{L}}_N$ of $\mathbb{L}_N^*$, and is thus given by the ratio of two (simple) quadratic forms in $\hat{\boldsymbol{\beta}}^n$. Note that $\widehat{S}^n$ does not depend on the value of σ^2.

5.2 Estimation of σ^2

The marginal distribution of $\mathbf{Y}_n$ given $\boldsymbol{\alpha}$ and σ^2 is normal $\mathscr{N}(\mathbf{R}_n\boldsymbol{\alpha}, \sigma^2(\boldsymbol{\Sigma}_n + \boldsymbol{\Psi}'_n\boldsymbol{\Lambda}'{\boldsymbol{\Psi}'_n}^T))$. With an improper prior on σ^2 (with density proportional to $1/\sigma^2$), its posterior distribution is inverse chi-square with $n-K$ degrees of freedom and such that $\mathsf{E}\{1/\sigma^2|\mathbf{Y}_n\} = 1/\hat{\sigma}_n^2$, with

$$\hat{\sigma}_n^2 = \frac{1}{n-K}\,(\mathbf{Y}_n - \mathbf{R}_n\hat{\boldsymbol{\alpha}}^n)^T(\boldsymbol{\Sigma}_n + \boldsymbol{\Psi}'_n\boldsymbol{\Lambda}'{\boldsymbol{\Psi}'_n}^T)^{-1}(\mathbf{Y}_n - \mathbf{R}_n\hat{\boldsymbol{\alpha}}^n)$$

(the restricted maximum likelihood estimator; see [32, p. 170]), where $\hat{\boldsymbol{\alpha}}^n$ corresponds to the K components of $\hat{\boldsymbol{\beta}}^n$ with indices in $\mathbb{K}$.

Given σ^2, the posterior distribution $\pi(\boldsymbol{\beta}|\mathbf{Y}_n, \sigma^2)$ of $\boldsymbol{\beta}$ is normal $\mathscr{N}(\hat{\boldsymbol{\beta}}^n,\, \sigma^2\,\mathbf{M}_n^{-1})$, with $\mathbf{M}_n$ given by (5.1). When the number of degrees of freedom, $n-K$, of the posterior distribution of σ^2 is large enough, we may consider that the posterior $\pi(\boldsymbol{\beta}|\mathbf{Y}_n)$ is normal $\mathscr{N}(\hat{\boldsymbol{\beta}}^n,\, \hat{\sigma}_n^2\,\mathbf{M}_n^{-1})$, and we shall make this assumption in the following. Notice in particular that $K = 1$ when all p_i equal zero, see Section 4.5.

5.3 Distribution of Sobol' indices

Take any index given by

$$S_{\widetilde{\mathbb{L}}_N}(\boldsymbol{\beta}) = \frac{\sum_{\underline{\ell}_k \in \widetilde{\mathbb{L}}_N} \beta^2_{\underline{\ell}_k}}{\sum_{k=2}^{M} \beta^2_{\underline{\ell}_k}} \tag{5.3}$$

for some $\widetilde{\mathbb{L}}_N \subseteq \mathbb{L}_N^*$ (which is well defined when $\beta_{\underline{\ell}_k} \neq 0$ for at least one $k > 1$, see (4.5)). We consider two different approximations of its posterior distribution. The first one (Section 5.3.1) is a normal approximation obtained via the delta-method; the second one (Section 5.3.2) is obtained from the exact distribution of a ratio of two quadratic forms in normal variables.

Remark 5.1. The value of $S_{\widetilde{\mathbb{L}}_N}(\boldsymbol{\beta})$ is invariant by a scale transformation of the $\beta_{\underline{\ell}_k}$, with the consequence that when $\boldsymbol{\beta}$ has the normal prior $\mathscr{N}(\mathbf{0}, \sigma^2\boldsymbol{\Lambda})$, the prior distribution of $S_{\widetilde{\mathbb{L}}_N}(\boldsymbol{\beta})$ does not depend on the value of σ^2. ◁

5.3.1 Normal approximation

Consider the ratio (5.3). Direct calculation gives

$$\frac{\partial S_{\widetilde{\mathbb{L}}_N}(\boldsymbol{\beta})}{\partial \boldsymbol{\beta}} = \frac{2}{\boldsymbol{\beta}^T\mathbf{J}\boldsymbol{\beta}}\,\boldsymbol{\Delta}_{\widetilde{\mathbb{L}}_N}\boldsymbol{\beta}\,, \tag{5.4}$$

with $\boldsymbol{\Delta}_{\widetilde{\mathbb{L}}_N}$ the diagonal matrix

$$\boldsymbol{\Delta}_{\widetilde{\mathbb{L}}_N} = \mathbf{U}_{\widetilde{\mathbb{L}}_N} - S_{\widetilde{\mathbb{L}}_N}\mathbf{J}\,, \tag{5.5}$$

where $\mathbf{U}_{\widetilde{\mathbb{L}}_N} = \mathrm{diag}\{u_{\underline{\ell}_k},\, k = 1, \ldots, M\}$, $u_{\underline{\ell}_k} = 1$ if $\underline{\ell}_k \in \widetilde{\mathbb{L}}_N$ and is zero otherwise, and $\mathbf{J}$ is the $M \times M$ diagonal matrix $\mathrm{diag}\{0, 1, \ldots, 1\}$. This yields a normal approximation of the posterior distribution $\pi(S_{\widetilde{\mathbb{L}}_N}(\boldsymbol{\beta})|\mathbf{Y}_n)$, with mean $S_{\widetilde{\mathbb{L}}_N}(\hat{\boldsymbol{\beta}}^n)$ and variance

$$V^n_{\widetilde{\mathbb{L}}_N} = \frac{4\,\hat{\sigma}_n^2}{[(\hat{\boldsymbol{\beta}}^n)^T\mathbf{J}\hat{\boldsymbol{\beta}}^n]^2}\,(\hat{\boldsymbol{\beta}}^n)^T\boldsymbol{\Delta}_{\widetilde{\mathbb{L}}_N}\mathbf{M}_n^{-1}\boldsymbol{\Delta}_{\widetilde{\mathbb{L}}_N}\hat{\boldsymbol{\beta}}^n\,, \tag{5.6}$$

from which we can construct approximate credible intervals for $S_{\widetilde{\mathbb{L}}_N}(\boldsymbol{\beta})$ (by simply considering critical values for the normal distribution, truncated to $[0,1]$). Notice that the estimation of Sobol' indices (5.3) and the construction of these credible intervals can be data-recursive; see also [12, 13] for another approach for first and second-order indices.

5.3.2 Exact posterior distribution of Sobol' indices for normal parameters

We can use the results in [16] and [3] to derive the exact distribution of $S_{\widetilde{\mathbb{L}}_N}(\boldsymbol{\beta})$ defined by (5.3) when $\boldsymbol{\beta}$ is normal $\mathcal{N}(\hat{\boldsymbol{\beta}}^n, \hat{\sigma}_n^2\,\mathbf{M}_n^{-1})$. Denoting $\mathbf{A} = \hat{\sigma}_n^2\,\mathbf{M}_n^{-1/2}\mathbf{U}_{\widetilde{\mathbb{L}}_N}\mathbf{M}_n^{-1/2}$ and $\mathbf{B} = \hat{\sigma}_n^2\,\mathbf{M}_n^{-1/2}\mathbf{J}\mathbf{M}_n^{-1/2}$, we get

$$\mathbb{F}_{\widetilde{\mathbb{L}}_N}(r) = \mathsf{Prob}\{S_{\widetilde{\mathbb{L}}_N}(\boldsymbol{\beta}) \le r\} = \mathsf{Prob}\{\mathbf{t}^T(\mathbf{A} - r\mathbf{B})\mathbf{t} \le 0\}\,,$$

where $\mathbf{t} \sim \mathcal{N}(\mathbf{0}, \mathbf{I}_M)$. Next, we construct the spectral decomposition $\mathbf{A} - r\mathbf{B} = \mathbf{P}\mathbf{D}\mathbf{P}^T$, with $\mathbf{D} = \mathrm{diag}\{\delta_1, \ldots, \delta_M\}$, and compute $\boldsymbol{\omega} = (\omega_1, \ldots, \omega_M)^T = \hat{\sigma}_n^{-1}\mathbf{P}^T\mathbf{M}_n^{1/2}\hat{\boldsymbol{\beta}}^n$. Then,

$$\mathbb{F}_{\widetilde{\mathbb{L}}_N}(r) = \frac{1}{2} - \frac{1}{\pi}\int_0^\infty \frac{\sin\beta(u)}{u\gamma(u)}\,\mathrm{d}u\,, \tag{5.7}$$

where

$$\beta(u) = \frac{1}{2}\sum_{k=1}^M \left[\arctan(\delta_k u) + \frac{\omega_k^2\delta_k u}{1+\delta_k^2u^2}\right] \quad \text{and} \quad \gamma(u) = \exp\left\{\frac{1}{2}\sum_{k=1}^M\left[\frac{\omega_k^2\delta_k^2u^2}{1+\delta_k^2u^2} + \frac{1}{2}\log(1+\delta_k^2u^2)\right]\right\}\,;$$

see [16]. The density of $S_{\widetilde{\mathbb{L}}_N}(\boldsymbol{\beta})$ is given by

$$f_{\widetilde{\mathbb{L}}_N}(r) = \frac{1}{\pi}\int_0^\infty \frac{\rho(u)\cos\beta(u) - u\delta(u)\sin\beta(u)}{2\gamma(u)}\,\mathrm{d}u\,, \tag{5.8}$$

where $\beta(u)$ and $\gamma(u)$ are defined above and

$$\rho(u) = \mathrm{trace}[\mathbf{H}\mathbf{F}^{-1}] + \boldsymbol{\omega}^T\mathbf{F}^{-1}(\mathbf{H} - u^2\mathbf{D}\mathbf{H}\mathbf{D})\mathbf{F}^{-1}\boldsymbol{\omega}\,,\ \delta(u) = \mathrm{trace}[\mathbf{H}\mathbf{D}\mathbf{F}^{-1}] + 2\,\boldsymbol{\omega}^T\mathbf{F}^{-1}\mathbf{H}\mathbf{D}\mathbf{F}^{-1}\boldsymbol{\omega}\,,$$

with $\mathbf{H} = \mathbf{P}^T\mathbf{B}\mathbf{P}$ and $\mathbf{F} = \mathbf{I}_M + u^2\mathbf{D}^2$; see [3].

Using the expressions (5.7) and (5.8) of $\mathbb{F}_{\widetilde{\mathbb{L}}_N}(r)$ and $f_{\widetilde{\mathbb{L}}_N}(r)$, we can easily construct credible intervals of minimum length for $S_{\widetilde{\mathbb{L}}_N}(\boldsymbol{\beta})$, e.g. via dichotomy search. For a given $\alpha \in (0,1)$, e.g., $\alpha = 0.05$, we find $b \in [0,1]$ such that $\mathbb{F}_{\widetilde{\mathbb{L}}_N}(b) - \mathbb{F}_{\widetilde{\mathbb{L}}_N}[a(b)] = 1-\alpha$, where $a(b) < b$ is such that $f_{\widetilde{\mathbb{L}}_N}[a(b)] = f_{\widetilde{\mathbb{L}}_N}(b)$ and is also determined by dichotomy search. An illustration is given in Figure 5-left. Of course, the required integral computations make this construction significantly heavier than when using the normal approximation of Section 5.3.1.

6 Experimental design

Suppose that we wish to estimate several indices $S_{\widetilde{\mathbb{L}}_{N,j}}(\boldsymbol{\beta})$, $j = 1, \ldots, J$, corresponding to different sets $\widetilde{\mathbb{L}}_{N,j} = \widetilde{\mathbb{L}}_N(\mathscr{U}_j)$ in (5.3). For instance, to estimate the d first-order total indices $\overline{S}_i$, $i = 1, \ldots, d$, we consider the d sets $\widetilde{\mathbb{L}}_{N,i} = \{\underline{\ell}_k \in \mathbb{L}_N^* : \ell_{k,i} \neq 0\}$; see Section 2.2. We then consider the $M \times J$ matrix

$$\mathbf{S}(\boldsymbol{\beta}) = \frac{2}{\boldsymbol{\beta}^T\mathbf{J}\boldsymbol{\beta}}\,\left[\boldsymbol{\Delta}_{\widetilde{\mathbb{L}}_{N,1}}\boldsymbol{\beta}\,|\,\cdots\,|\,\boldsymbol{\Delta}_{\widetilde{\mathbb{L}}_{N,J}}\boldsymbol{\beta}\right] \tag{6.1}$$

formed from the derivatives (5.4) of the J indices of interest. Following developments similar to those in Section 5.3.1, we can approximate the posterior joint distribution of $S_{\widetilde{\mathbb{L}}_{N,1}}, \dots, S_{\widetilde{\mathbb{L}}_{N,J}}$ by a normal distribution with covariance matrix $\hat{\sigma}^2_n \mathbf{S}^T(\hat{\boldsymbol{\beta}}^n)\mathbf{M}_n^{-1}\mathbf{S}(\hat{\boldsymbol{\beta}}^n)$, and a good experimental design $\mathscr{D}_n$ should minimise a scalar function of $\mathbf{S}^T(\hat{\boldsymbol{\beta}}^n)\mathbf{M}_n^{-1}\mathbf{S}(\hat{\boldsymbol{\beta}}^n)$. We suppose that $\mathscr{D}_n \subset \mathscr{X}_Q = \{\mathbf{x}^{(1)}, \dots, \mathbf{x}^{(Q)}\}$, a given finite set of candidate points, see Remark 4.3.

Unsurprisingly, due to the nonlinear dependence of $S_{\widetilde{\mathbb{L}}_{N,j}}(\boldsymbol{\beta})$ in $\boldsymbol{\beta}$, an optimal experiment for the estimation of the $S_{\widetilde{\mathbb{L}}_{N,j}}(\boldsymbol{\beta})$ depends on the unknown $\boldsymbol{\beta}$; see, for instance, [26, Chap. 8]. This difficulty can be circumvented in different ways. The approach of Section 6.1 is adaptive: after n_0 evaluations at some prespecified design $\mathscr{D}_{n_0}$ (for instance, a space-filling design in $\mathscr{X}$; see, e.g., [25]), the next design points are chosen sequentially, the choice of $\mathbf{x}_{n+1}$ for $n \geq n_0$ being based on the current estimated value $\hat{\boldsymbol{\beta}}^n$. A batch-sequential construction can also be used, where the estimated value $\hat{\boldsymbol{\beta}}^{kn_0}$ is used for the selection of $\mathbf{x}_{kn_0+1}, \dots, \mathbf{x}_{(k+1)n_0}$. Here all batches have the same size n_0, but extension to more general situations is straightforward; in particular, two-stage design uses $\hat{\boldsymbol{\beta}}^{n_0}$ for the construction of all $\mathbf{x}_n$ for $n > n_0$. One may alternatively try to design each batch of points optimally (Section 6.2), either with an exchange-type algorithm (Section 6.2.1) or using the classical machinery of approximate design theory to construct an optimal design measure ξ^* through the solution of a convex programming problem, see [23], from which an exact design can be extracted. This is considered in Section 6.2.2.

6.1 Adaptive design

Denote by $\boldsymbol{\Omega}_n(\boldsymbol{\beta})$ the $J \times J$ matrix

$$\boldsymbol{\Omega}_n(\boldsymbol{\beta}) = \mathbf{S}^T(\boldsymbol{\beta})\mathbf{M}_n^{-1}\mathbf{S}(\boldsymbol{\beta})\,,$$

with $\mathbf{S}(\boldsymbol{\beta})$ given by (6.1), so that $\boldsymbol{\Omega}_n(\hat{\boldsymbol{\beta}}^n)$ characterises the precision of the estimation of the J indices $S_{\widetilde{\mathbb{L}}_{N,j}}(\boldsymbol{\beta})$ of interest, $j = 1, \dots, J$, after n evaluations of $\mathfrak{f}(\cdot)$.

The choice of suitable design criteria depends on which aspect of the precision we consider more appealing. Assuming that the indices of interest are approximately normally distributed, the D-optimality criterion $\det(\boldsymbol{\Omega}_n)$ is related to the (squared) volume of joint confidence ellipsoids; the A-optimality criterion $\mathrm{trace}(\boldsymbol{\Omega}_n)$ is related to the sum of squared lengths of the principal axes of these ellipsoids; MV-optimality aims at minimising the maximum of the variances of individual indices, and the criterion is given by $\max[\mathrm{diag}(\boldsymbol{\Omega}_n)]$; see [18].

D-optimality for the estimation of first-order Sobol' indices in PCE models is considered in [4], and we follow the same line in the more general framework considered here. We suppose that n_0 evaluations of $\mathfrak{f}(\cdot)$ have been performed, such that $\mathbf{M}_{n_0}$ is nonsingular. Then, for any $n \geq n_0$, after estimation of $\hat{\boldsymbol{\beta}}^n$ from n evaluations of $\mathfrak{f}(\cdot)$, we choose the next design point $\mathbf{x}_{n+1}$ which yields the largest decrease of $j[\boldsymbol{\Omega}_{n+1}(\hat{\boldsymbol{\beta}}^n)]$, with $H(\cdot)$ one of the criteria above.

Straightforward calculations indicate that

$$\mathbf{x}_{n+1} = \arg\max_{\mathbf{x}\in\mathscr{X}_Q} \frac{\boldsymbol{\psi}^T(\mathbf{x})\mathbf{M}_n^{-1}\mathbf{S}(\hat{\boldsymbol{\beta}}^n)[\mathbf{S}^T(\hat{\boldsymbol{\beta}}^n)\mathbf{M}_n^{-1}\mathbf{S}(\hat{\boldsymbol{\beta}}^n)]^{-1}\mathbf{S}^T(\hat{\boldsymbol{\beta}}^n)\mathbf{M}_n^{-1}\boldsymbol{\psi}(\mathbf{x})}{s^2(\mathbf{x}) + \boldsymbol{\psi}^T(\mathbf{x})\mathbf{M}_n^{-1}\boldsymbol{\psi}(\mathbf{x})} \tag{6.2}$$

when minimising $\det[\boldsymbol{\Omega}_{n+1}(\hat{\boldsymbol{\beta}}^n)]$,

$$\mathbf{x}_{n+1} = \arg\max_{\mathbf{x}\in\mathscr{X}_Q} \frac{\boldsymbol{\psi}^T(\mathbf{x})\mathbf{M}_n^{-1}\mathbf{S}(\hat{\boldsymbol{\beta}}^n)\mathbf{S}^T(\hat{\boldsymbol{\beta}}^n)\mathbf{M}_n^{-1}\boldsymbol{\psi}(\mathbf{x})}{s^2(\mathbf{x}) + \boldsymbol{\psi}^T(\mathbf{x})\mathbf{M}_n^{-1}\boldsymbol{\psi}(\mathbf{x})} \tag{6.3}$$

when minimising trace$[\boldsymbol{\Omega}_{n+1}(\hat{\boldsymbol{\beta}}^n)]$, and

$$\mathbf{x}_{n+1} = \arg\max_{\mathbf{x}\in\mathscr{X}_Q} \min_{j=1,\ldots,J} \left\{ \frac{[\boldsymbol{\psi}^T(\mathbf{x})\mathbf{M}_n^{-1}\mathbf{S}(\hat{\boldsymbol{\beta}}^n)\mathbf{e}_j]^2}{s^2(\mathbf{x}) + \boldsymbol{\psi}^T(\mathbf{x})\mathbf{M}_n^{-1}\boldsymbol{\psi}(\mathbf{x})} - \mathbf{e}_j^T\mathbf{S}^T(\hat{\boldsymbol{\beta}}^n)\mathbf{M}_n^{-1}\mathbf{S}(\hat{\boldsymbol{\beta}}^n)\mathbf{e}_j \right\} \tag{6.4}$$

when minimising $\max\{\text{diag}[\boldsymbol{\Omega}_{n+1}(\hat{\boldsymbol{\beta}}^n)]\}$, with $\boldsymbol{\psi}(\mathbf{x}) = [\psi_{\underline{\ell}_1}(\mathbf{x}), \ldots, \psi_{\underline{\ell}_M}(\mathbf{x})]^T$ and $\mathbf{e}_j$ the jth canonical basis vector of $\mathbb{R}^J$. Note that we may also consider weighed versions of the criteria trace$(\boldsymbol{\Omega})$ and $\max[\text{diag}(\boldsymbol{\Omega})]$ by introducing weights along the diagonal of $\boldsymbol{\Omega}$, for instance in order to consider individual relative precision of the J indices.

Remark 6.1. The presence of independent errors in the model (3.10) has the consequence that the sequential construction above may yield repetitions of observations at the same design point When this happens, it may be interpreted as an indication that the approximations involved are too rough for the number of observations considered and should be refined by (i) considering a finer set $\mathscr{X}_Q$ and/or (ii) enlarging the number of components in (3.10), that is, the value of N in (4.5). Repetitions can always be avoided by considering that $s^2(\mathbf{x})$ is infinite for any $\mathbf{x}$ already selected. ◁

6.2 Optimal design

A locally D, A or MV-optimal n-point exact design $\mathscr{D}_n(\boldsymbol{\beta}_0)$ is obtained by direct minimisation of $j[\boldsymbol{\Omega}_n(\boldsymbol{\beta}_0)]$ with respect to $\mathscr{D}_n$, for one of the criteria mentioned above and for a given nominal value $\boldsymbol{\beta}_0$ of $\boldsymbol{\beta}$. This is generally a formidable problem (non-convex, with multiple local minima) when n and d are large, and the usual approach is to resort to an exchange type algorithm, like the one considered in Section 6.2.1. Another approach (Section 6.2.2) is to construct an optimal design measure ξ^* (a probability measure on $\mathscr{X}$) and then extract an exact design from the support of ξ^*. We only consider A-optimality in the following.

Direct calculation shows that trace$[\boldsymbol{\Omega}_n(\boldsymbol{\beta}_0)]$ (to be minimised) is proportional to

$$H[\boldsymbol{\Omega}_n(\boldsymbol{\beta}_0)] = \text{trace}\left[\mathbf{C}(\boldsymbol{\beta}_0)\mathbf{M}_n^{-1}\right] ,$$

where

$$\mathbf{C}(\boldsymbol{\beta}) = \sum_{j=1}^{J} \boldsymbol{\Delta}_{\widetilde{\mathbb{L}}_{N,j}}(\boldsymbol{\beta})\, \boldsymbol{\beta}\boldsymbol{\beta}^T\, \boldsymbol{\Delta}_{\widetilde{\mathbb{L}}_{N,j}}(\boldsymbol{\beta}) , \tag{6.5}$$

and where the $\boldsymbol{\Delta}_{\widetilde{\mathbb{L}}_{N,j}}(\boldsymbol{\beta})$ are given by (5.5) (they depend on $\boldsymbol{\beta}$ through the indices $S_{\widetilde{\mathbb{L}}_{N,i}}(\boldsymbol{\beta}) = (\boldsymbol{\beta}^T\mathbf{U}_{\widetilde{\mathbb{L}}_{N,i}}\boldsymbol{\beta})/(\boldsymbol{\beta}^T\mathbf{J}\boldsymbol{\beta})$, see (5.3)). Note that $\{\mathbf{C}(\boldsymbol{\beta})\}_{1,1} = 0$.

In batch sequential design, $\boldsymbol{\beta}_0$ in $\mathbf{C}(\boldsymbol{\beta}_0)$ is set to the current estimated value $\hat{\boldsymbol{\beta}}^n$. It is also tempting to try to construct an initial optimal design before any evaluation of $\mathfrak{f}(\cdot)$, i.e., in situations where no prior value $\boldsymbol{\beta}_0$ is available. One may then replace all quadratic forms in $\boldsymbol{\beta}$ that appear in $H[\boldsymbol{\Omega}_n(\boldsymbol{\beta})]$ by their expectations, with $\boldsymbol{\beta}$ normally distributed $\mathscr{N}(\mathbf{0}, \sigma^2\boldsymbol{\Lambda})$. Direct calculations shows that this amounts to replacing $\boldsymbol{\Omega}_n(\boldsymbol{\beta}_0)$ by $\widetilde{\boldsymbol{\Omega}}_n$, with

$$\{\widetilde{\boldsymbol{\Omega}}_n\}_{i,j} = \frac{4}{\sigma^2\ \text{trace}^2(\mathbf{J}\boldsymbol{\Lambda})}\ \text{trace}\left[\mathbf{M}_n^{-1}\boldsymbol{\Delta}_{\widetilde{\mathbb{L}}_{N,i}}(\widetilde{\boldsymbol{\beta}})\boldsymbol{\Delta}_{\widetilde{\mathbb{L}}_{N,j}}(\widetilde{\boldsymbol{\beta}})\boldsymbol{\Lambda}\right] ,$$

where we have denoted $\widetilde{\boldsymbol{\beta}} = \text{diag}\{\Lambda_{\underline{\ell}_k}^{1/2}, k = 1, \ldots, M\}$. We then minimise $H(\widetilde{\boldsymbol{\Omega}}_n) = \text{trace}[\widetilde{\mathbf{C}}\mathbf{M}_n^{-1}]$ with

$$\widetilde{\mathbf{C}} = \boldsymbol{\Lambda} \sum_{j=1}^{J} \boldsymbol{\Delta}^2_{\widetilde{\mathbb{L}}_{N,j}}(\widetilde{\boldsymbol{\beta}}) , \tag{6.6}$$

where we used the fact that $\mathbf{\Lambda}$ and the $\mathbf{\Delta}_{\widetilde{\mathbb{L}}_{N,j}}$ are diagonal. Note that $\{\widetilde{\mathbf{C}}\}_{1,1} = 0$ and $\{\widetilde{\mathbf{C}}\}_{k,k} > 0$ for $k \geq 2$ (since $S_{\widetilde{\mathbb{L}}_{N,i}}(\widetilde{\boldsymbol{\beta}}) > 0$ for all i, so that $\{\mathbf{\Delta}_{\widetilde{\mathbb{L}}_{N,i}}(\widetilde{\boldsymbol{\beta}})\}_{k,k} \neq 0$ for all $k \geq 2$, see (5.5)).

6.2.1 An exchange algorithm for exact design

Instead of considering the direct minimisation of trace$[\mathbf{C}\mathbf{M}_n^{-1}]$ with respect to $\mathscr{D}_n$, with $\mathbf{C} = \mathbf{C}(\boldsymbol{\beta}_0)$ given by (6.5) for some $\boldsymbol{\beta}_0$ in batch sequential design, or $\mathbf{C} = \widetilde{\mathbf{C}}$ given by (6.6) in the construction of an initial design, we consider an exchange-type algorithm, similar to the DETMAX algorithm of [21]. Let $\mathscr{D}_n = \mathscr{D}_n^{(k)}$ denote the current design at iteration k of the algorithm and $\mathbf{M}_n$ denote the corresponding Bayesian information matrix. We suppose that $\mathscr{D}_n$ is such that $\mathbf{M}_n$ is nonsingular. Each iteration comprises two steps. We only consider excursions through $(n+1)$-point designs, but excursions through designs of size larger than $n+1$ could be considered as well.

First, we consider an optimal design augmentation, obtained by adding the point

$$\mathbf{x}_{n+1} = \arg\max_{\mathbf{x}\in\mathscr{X}_Q} \frac{\boldsymbol{\psi}^T(\mathbf{x})\mathbf{M}_n^{-1}\mathbf{C}\mathbf{M}_n^{-1}\boldsymbol{\psi}(\mathbf{x})}{s^2(\mathbf{x}) + \boldsymbol{\psi}^T(\mathbf{x})\mathbf{M}_n^{-1}\boldsymbol{\psi}(\mathbf{x})} \tag{6.7}$$

to $\mathscr{D}_n$, where we set $s^2(\mathbf{x}_i) = \infty$ for all $\mathbf{x}_i \in \mathscr{D}_n$ to avoid repetitions of observations at the same point.

Second, we return to an n-point design by removing a point from $\mathscr{D}_n^+ = \mathscr{D}_n \cup \{\mathbf{x}_{n+1}\}$. Denote by $\mathbf{M}_n^+$ the Bayesian information matrix corresponding to $\mathscr{D}_n^+$. It satisfies

$$(\mathbf{M}_n^+)^{-1} = \mathbf{M}_n^{-1} - \frac{\mathbf{M}_n^{-1}\boldsymbol{\psi}(\mathbf{x}_{n+1})\boldsymbol{\psi}^T(\mathbf{x}_{n+1})\mathbf{M}_n^{-1}}{s^2(\mathbf{x}_{n+1}) + \boldsymbol{\psi}^T(\mathbf{x}_{n+1})\mathbf{M}_n^{-1}\boldsymbol{\psi}(\mathbf{x}_{n+1})}\,,$$

and elementary calculation shows that the optimal choice for the point $\mathbf{x}_-$ to be removed is given by

$$\mathbf{x}_- = \arg\min_{\mathbf{x}\in\mathscr{D}_n^+} \frac{\boldsymbol{\psi}^T(\mathbf{x})(\mathbf{M}_n^+)^{-1}\mathbf{C}(\mathbf{M}_n^+)^{-1}\boldsymbol{\psi}(\mathbf{x})}{s^2(\mathbf{x}) - \boldsymbol{\psi}^T(\mathbf{x})(\mathbf{M}_n^+)^{-1}\boldsymbol{\psi}(\mathbf{x})}\,.$$

The design $\mathscr{D}_n^{(k+1)}$ for next iteration is then $\mathscr{D}_n \cup \{\mathbf{x}_{n+1}\} \setminus \{\mathbf{x}_-\}$. The algorithm is stopped when $H(\cdot)$ does not decrease between two successive iterations, which generally means that $\mathbf{x}_- = \mathbf{x}_{n+1}$.

6.2.2 Exact design via optimal design measures

Construction of an optimal design measure. Let Ξ denote the set of probability measure on $\mathscr{X}_Q$, a finite subset of $\mathscr{X}$. Consider the construction of an optimal initial design. For any ξ in Ξ and any $\vartheta \in \mathbb{R}^+$, define

$$\mathbf{M}_\vartheta(\xi) = \int_{\mathscr{X}_Q} \frac{1}{s^2(\mathbf{x})}\,\boldsymbol{\psi}(\mathbf{x})\boldsymbol{\psi}^T(\mathbf{x})\,\mathrm{d}\xi(\mathbf{x}) + \frac{\mathbf{\Lambda}_0^{-1}}{\vartheta}\,, \tag{6.8}$$

so that $n\,\mathbf{M}_n(\mu_n) = \mathbf{M}_n$ given by (5.1) when $\mu_n = (1/n)\sum_{k=1}^n \delta_{\mathbf{x}_i}$ is the empirical measure associated with the design $\mathscr{D}_n$. An optimal design measure ξ^* is obtained by minimizing the L-optimality criterion (L for linear)

$$H_\vartheta(\xi) = \mathrm{trace}\left[\mathbf{C}\mathbf{M}_\vartheta^{-1}(\xi)\right]\,, \tag{6.9}$$

with $\mathbf{C} = \widetilde{\mathbf{C}}$ given by (6.6), with respect to $\xi \in \Xi$. In batch sequential design, we would take $\mathbf{C} = \mathbf{C}(\hat{\boldsymbol{\beta}}^n)$ given by (6.5) for the current estimated value $\hat{\boldsymbol{\beta}}^n$ and substitute $\mathbf{M}_n$ for $\mathbf{\Lambda}_0^{-1}$ in (6.8). Since $\mathscr{X}_Q$ is finite, the minimisation of $H_\vartheta(\xi)$ forms a finite-dimensional convex optimisation

problem, for which many efficient algorithms are available; see, e.g., [26, Chap. 9]. Iteration k of a vertex-direction algorithm transfers some mass to $\mathbf{x}^* \in \mathscr{X}_Q$ that minimises the current directional derivative $F_\vartheta(\xi^k, \mathbf{x})$, here given by

$$\begin{aligned} F_\vartheta(\xi^k, \mathbf{x}) &= \lim_{\gamma \to 0^+} \frac{H_\vartheta[(1-\gamma)\xi^k + \gamma\delta_{\mathbf{x}}] - H_\vartheta(\xi^k)}{\gamma} \\ &= -\frac{\boldsymbol{\psi}^T(\mathbf{x})\mathbf{M}_\vartheta^{-1}(\xi^k)\mathbf{C}\mathbf{M}_\vartheta^{-1}(\xi^k)\boldsymbol{\psi}(\mathbf{x})}{s^2(\mathbf{x})} + \operatorname{trace}\left\{\mathbf{M}_\vartheta^{-1}(\xi^k)[\mathbf{M}_\vartheta(\xi^k) - \frac{\boldsymbol{\Lambda}_0^{-1}}{\vartheta}]\mathbf{M}_\vartheta^{-1}(\xi^k)\mathbf{C}\right\} . \end{aligned}$$

This gives $\mathbf{x}^* = \arg\max_{\mathbf{x}\in\mathscr{X}_Q}[\boldsymbol{\psi}^T(\mathbf{x})\mathbf{M}_\vartheta^{-1}(\xi^k)\mathbf{C}\mathbf{M}_\vartheta^{-1}(\xi^k)\boldsymbol{\psi}(\mathbf{x})]/s^2(\mathbf{x})$, compare with (6.7). Note that we have assumed that $\mathbf{M}_\vartheta(\xi^k)$ is nonsingular. This can always be achieved trough regularisation, by re-introducing a weakly informative prior $\mathscr{N}(\mathbf{0}, \gamma^2\,\mathbf{I}_K)$ on the K parameters $\boldsymbol{\alpha}$, with a large γ, so that all diagonal terms of $\boldsymbol{\Lambda}_0^{-1}$ become strictly positive in (6.8).

Extraction of an exact design. Let ξ^* denote an ϵ-optimal design measure for the criterion $H_\vartheta(\cdot)$, satisfying $\min_{\mathbf{x}\in\mathscr{X}_Q} F_\vartheta(\xi^*, \mathbf{x}) > -\epsilon$, with ϵ a small positive number. The measure ξ^* is a discrete measure with a finite number N^* of support points, and can be written as

$$\xi^* = \xi_{N^*} = \sum_{k=1}^{N^*} w_{k:N^*}\delta_{\mathbf{x}_k} ,$$

where the weights are ordered by decreasing values: $w_{1:N^*} \geq w_{2:N^*} \geq \cdots \geq w_{N^*:N^*}$. Our extraction procedure consists in sequentially reducing the support by transferring the smallest current weight to another support point, suitably chosen (see also Algorithm 1 of [11] for an alternative approach). The size n of the design extracted is not set *a priori*, but is in some sense adapted to the truncation level used to construct the set $\mathbb{L}_N$, see (4.5). The value of ϑ used to construct ξ^* should be of the same order of magnitude as N, but this choice is not critical. For ξ_N a discrete measure of the form $\xi_N = \sum_{k=1}^N w_k\delta_{\mathbf{x}_k}$, we denote by $\xi_{N,u}$ the uniform measure having the same support; that is, $\xi_{N,u} = (1/N)\sum_{k=1}^N \delta_{\mathbf{x}_k}$. The matrix $N\mathbf{M}_N(\xi_{N,u})$ thus corresponds to the Bayesian information matrix $\mathbf{M}_N$ for the design $\mathscr{D}_N$ formed by the support of ξ_N, see (5.1). The construction is described in Algorithm 1.

Algorithm 1 Greedy algorithm for merging support points

Require: ξ_{N^*}, an ϵ-optimal design measure for $H_\vartheta(\cdot)$, a threshold $\tau > 1$;

1: set $N = N^*$;
2: **while** $N > 1$ **do**
3: compute $k^* = \arg\max_{k=1,\ldots,N-1}[\boldsymbol{\psi}^T(\mathbf{x}_k)\mathbf{M}_\vartheta^{-1}(\xi_N)\mathbf{C}\mathbf{M}_\vartheta^{-1}(\xi_N)\boldsymbol{\psi}(\mathbf{x}_k)]/s^2(\mathbf{x}_k)$;
4: Compute $\xi_{N-1} = \sum_{k=1}^{N-1} w_{k,N}\delta_{\mathbf{x}_k}$ where $w_{k,N} = w_{k:N}$ for $k \neq k^*$ and $w_{k^*,N} = w_{k^*:N} + w_{N:N}$; reorder the weights of ξ_{N-1} by decreasing values, i.e., write $\xi_{N-1} = \sum_{k=1}^{N-1} w_{k:N-1}\delta_{\mathbf{x}_k}$, with $w_{1:N-1} \geq w_{2:N-1} \geq \cdots \geq w_{N-1:N-1}$; $N \leftarrow N-1$;
5: if $\rho_N = \operatorname{trace}\{\mathbf{C}[N\mathbf{M}_N(\xi_{N,u})]^{-1}\}/\operatorname{trace}\{\mathbf{C}[(N+1)\mathbf{M}_{N+1}([N/(N+1)]\xi_{N+1,u})]^{-1}\} > \tau$, stop;
6: **end while**
7: **return** $n = N+1$ and $\mathscr{D}_n$ given by the support of ξ_{N+1}.

We rescale $\xi_{N+1,u}$ into $[N/(N+1)]\xi_{N+1,u}$ in the test at line 5 of the algorithm, since $\xi_{N+1,u}$ has one more point than $\xi_{N,u}$ (and thus $\operatorname{trace}\{\mathbf{C}[N\mathbf{M}_N(\xi_{N,u})]^{-1}\} > \operatorname{trace}\{\mathbf{C}[(N+1)\mathbf{M}_{N+1}(\xi_{N+1,u})]^{-1}\}$ for all N), whereas ρ_N usually fluctuates around 1 in the first steps with N close to N^*; see Figure 13-right in Section 7 for an illustration. We can also base the selection of an optimal k^* at line 3 on

the comparison between the values of $H_\vartheta(\cdot)$, or $H_N(\cdot)$, achieved for all the $N-1$ possible mass transfers, at the expense of a significantly larger computational cost when N^* is large.

7 Numerical examples

7.1 Ishigami function

This function depends on three variables and is frequently used as a test-case in sensitivity analysis. It is given by $\mathfrak{f}(\mathbf{x}) = \sin(x_1) + a\sin^2(x_2) + bx_3^4\sin(x_1)$, $\mathbf{x}$ being uniformly distributed in $\mathscr{X} = [-\pi, \pi]^3$. We shall use the values $a = 7$ and $b = 0.1$. The first-order indices are equal to

$$S_1 = (b\pi^4/5 + b^2\pi^8/50 + 1/2)/\Delta\,,\ S_2 = a^2/(8\Delta)\,, S_3 = 0$$

where $\Delta = a^2/8 + b\pi^4/5 + b^2\pi^8/18 + 1/2$, the second-order indices are all zero excepted $S_{1,3} = 8b^2\pi^8/(225\Delta)$. We have, by definition, see Section 2.1,

$$\overline{S}_1 = S_1 + S_{1,3}\,,\ \overline{S}_2 = S_2\,,\ \overline{S}_3 = S_{1,3}\,,\ \underline{S}_{1,2} = S_1 + S_2\,,\ \underline{S}_{1,3} = S_{1,3} + S_1 \text{ and } \underline{S}_{2,3} = S_2\,.$$

We approximate each marginal of μ by the discrete uniform measure that puts weight $1/100$ at each of the points $(j-1)/99$, $j = 1, \ldots, q = 100$ and use the covariance $K_{3/2}(x, y; \theta)$, see Section 4.6. We set $p_i = 0$ for $i = 1, 2, 3$ (we have observed that the performances are significantly deteriorated when setting the polynomial degrees p_i to positive values). We estimate the indices by evaluating $\mathfrak{f}(\cdot)$ at the first n points of Sobol' low-discrepancy sequence in $[0, 1]^3$, and take $N = n$ in (4.5).

Figure 4-left shows the density (5.8) of the prior distribution of first-order indices S_i (the same for $i = 1, 2, 3$) for $\theta = 2$ (solid line) and $\theta = 20$ (dashed line). Figure 4-right shows the two posterior distributions obtained for S_1 when $n = 64$, $\theta = 2$ (solid line) and $\theta = 20$ (dashed line), $\boldsymbol{\beta}$ having the normal distribution $\mathscr{N}(\hat{\boldsymbol{\beta}}^n, \hat{\sigma}_n^2\,\mathbf{M}_n^{-1})$; see Section 5.3.2. The true value of S_1 is about 0.3139; the model with $\theta = 2$ seems able to adequately capture the global behaviour of $\mathfrak{f}(\cdot)$, whereas prior weights on components with fast variations are exaggeratedly large when $\theta = 20$, see the discussion in Section 4.6, which makes the estimation less precise.

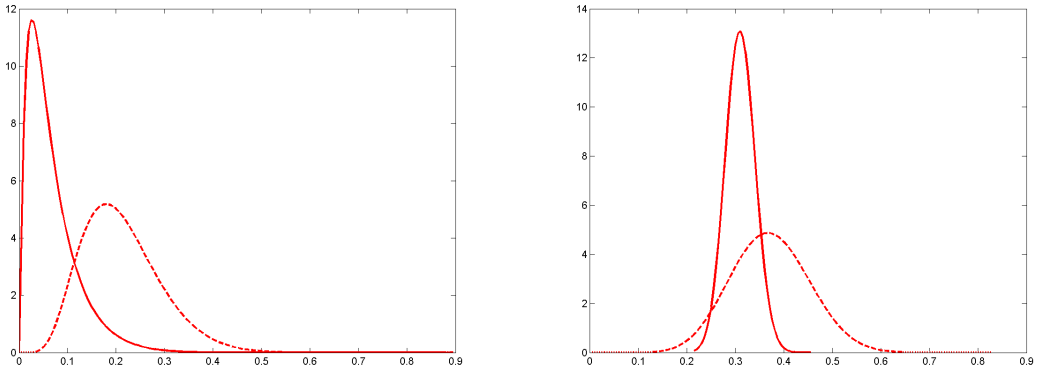

Figure 4: Ishigami function. Left: density (5.8) for S_i (first-order indices) when $\boldsymbol{\beta}$ has the prior distribution $\mathscr{N}(\mathbf{0}, \sigma^2\boldsymbol{\Lambda})$ (see Remark 5.1). Right: density of S_1 when $\boldsymbol{\beta}$ has the posterior distribution $\mathscr{N}(\hat{\boldsymbol{\beta}}^n, \hat{\sigma}_n^2\,\mathbf{M}_n^{-1})$, $n = 64$. The covariance for univariate models is $K_{3/2}(x, y; 2)$ (solid line) or $K_{3/2}(x, y; 20)$ (dashed line); $S_1 \simeq 0.3139$.

Figure 5-left shows the posterior density (5.8) for S_1 (solid line, same as in Figure 4-right), the minimum-length 95% credible interval, and the normal approximation of the posterior (dashed line), all for $\theta = 2$. Figure 5-right shows the posterior density (5.8) of $S_{1,2}$ (solid line) and its normal approximation (dashed line). Figure 6 presents the same information for $S_{1,3}$, when $n = 64$ (left) and $n = 256$ (right). The estimated value $\widehat{S}_1^n$ given by (5.2) equals 0.3337 and is reasonably close to the true value $S_1 \simeq 0.3139$, both the exact posterior and its normal approximation yield 95% credible intervals that contain S_1, see Figure 5-left. The estimation of second-order indices is more difficult with $n = 64$: $S_{1,2}$ tends to be over-estimated (Figure 5-right) and $S_{1,3}$ underestimated (Figure 6-left), although the situation improves when increasing n (Figure 6-right).

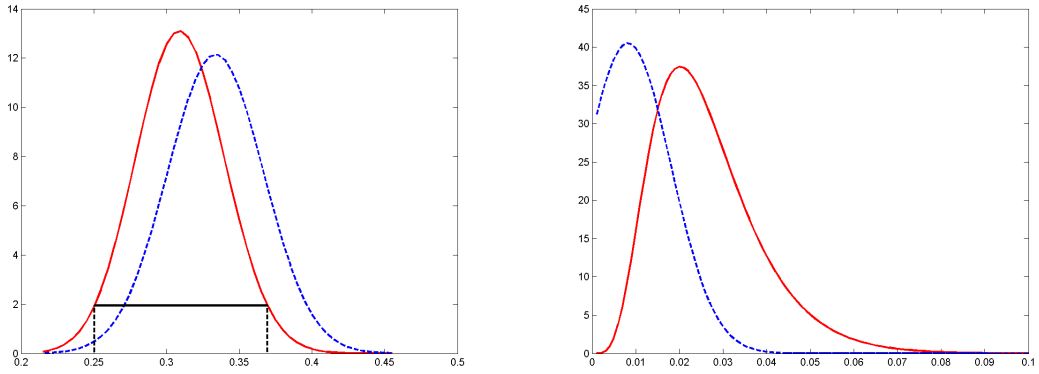

Figure 5: Ishigami function: posterior distributions for $n = 64$ with covariance $K_{3/2}(x, y; 2)$. Left: posterior density (5.8) for S_1 (solid line) and minimum-length 95% credible interval; normal approximation (dashed line); $S_1 \simeq 0.3139$. Right: posterior density (5.8) for $S_{1,2}$ (solid line) and its normal approximation (dashed line); the true value is zero.

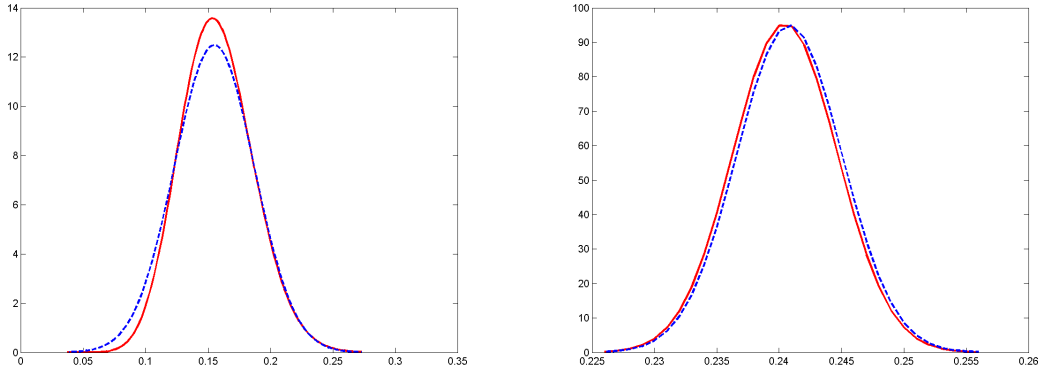

Figure 6: Ishigami function: posterior density (5.8) for $S_{1,3}$ (solid line) and its normal approximation (dashed line) with covariance $K_{3/2}(x, y; 2)$. Left: $n = 64$; Right: $n = 256$; $S_{1,3} \simeq 0.2437$.

Figure 7-left show the evolution of first order-index $\widehat{S}_1^n$, see (5.2), with $\hat{\boldsymbol{\beta}}^n$ estimated from evaluations at successive points of Sobol' sequence. After a batch of $n_0 = 10$ evaluations, we use a recursive construction for $\hat{\boldsymbol{\beta}}^n$, and thus for $\widehat{S}_1^n$, for $n = 11, \ldots, 256$ (dashed line). The 95% credible

intervals for the normal approximation (Section 5.3.1) are shown in dashed line, the true value of S_1 corresponds to the horizontal solid line. Figure 7-right presents the same information for S_2 (top) and S_3 (bottom). We have taken $\theta = 2$ in $K_{3/2}(x, y; \theta)$, $N = 256$ in (4.5) and $p_i = 0$ for $i = 1, 2, 3$.

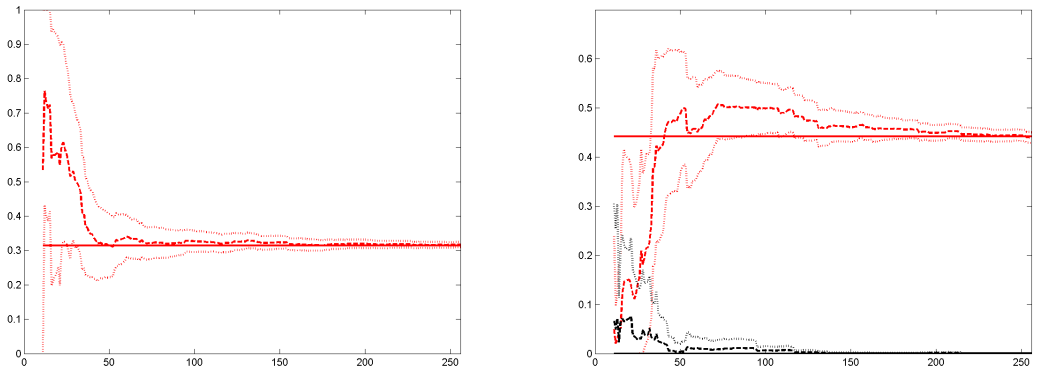

Figure 7: Ishigami function: estimated first-order indices (dashed line) and normal approximation of 95% credible intervals (dotted lines) with a tensorised BLM using $K_{3/2}(x, y; 2)$; the solid line indicates the true value. Left: S_1; right: S_2 (top) and S_3 (bottom).

The function $\mathfrak{f}(\cdot)$ is fixed, but we may consider the variability of estimated indices when using different designs. We take $\theta = 2$ in $K_{3/2}(x, y; \theta)$, $N = n$ in (4.5) and $p_i = 0$ for $i = 1, 2, 3$ in the construction of the tensorised BLM, and evaluate $\mathfrak{f}(\cdot)$ at 100 different n-point Lh designs $\mathscr{D}_n^{(k)}$ constructed as follows. We first generate 10,000 random Lh designs in $\mathscr{X}$, and then select the 100 designs having the smallest value of $J_q(\cdot)$ defined by

$$J_q(\mathscr{D}_n) = \sum_{i=1}^{n} \min_{j \neq i} \|\mathbf{x}_j - \mathbf{x}_i\|^q \,, \; q < 0 \,,$$

with $\mathscr{D}_n = \{\mathbf{x}_1, \ldots, \mathbf{x}_n\}$. $J_q^{1/q}(\mathscr{D}_n)$ tends to $J_{Mm}(\mathscr{D}_n) = \min_{i \neq j} \|\mathbf{x}_j - \mathbf{x}_i\|$ as q tends to $-\infty$, but its value depends on the respective positions of all points, contrary to the maximin criterion $J_{Mm}(\cdot)$. A design optimal for $J_q(\cdot)$ is $n^{1/q}$-efficient for $J_{Mm}(\cdot)$ in the family considered [24]; we take $q = -20$ to select designs having good space-filling properties. The left column of Figure 8 presents box-plots (median, 25th and 75th percentiles and minimum and maximum values) of the errors $\widehat{S}^n - S$, for $n = 64$ (top), 128 (middle) and 256 (bottom) respectively, for first-order, total, second-order and closed-second-order indices. We can see that the estimation is already reasonably accurate for small n. Table 3 gives the empirical coverage probabilities (in %), for the 100 random Lh designs, of approximate 2σ credible intervals constructed with the variance $V^n_{\mathbb{L}_N}$ given by (5.6), for first-order indices (S_1, S_2, S_3), total indices $(\overline{S}_1, \overline{S}_2, \overline{S}_3)$, second-order indices $(S_{1,2}, S_{1,3}, S_{2,3})$ and closed-second-order indices $(\underline{S}_{1,2}, \underline{S}_{1,3}, \underline{S}_{2,3})$. Although $V^n_{\mathbb{L}_N}$ accounts for uncertainty due to the possible variability of $\mathfrak{f}(\cdot)$ conditional to evaluations at a fixed design, by considering different designs of the same type (they are all space-filling and have the same one-dimensional projections) we try to mimic the behaviour of different $\mathfrak{f}(\cdot)$ for the same design. The coverage probabilities in Table 3 are acceptable in most cases (the small values observed for $S_{1,3}$ can be explained by the presence of a small estimation bias, see Figure 8).

We now consider estimation of indices via (Legendre) polynomial-chaos expansion. When the total polynomial degree is D, the model contains $M = \binom{D+d}{d}$ parameters. Figure 9 presents the

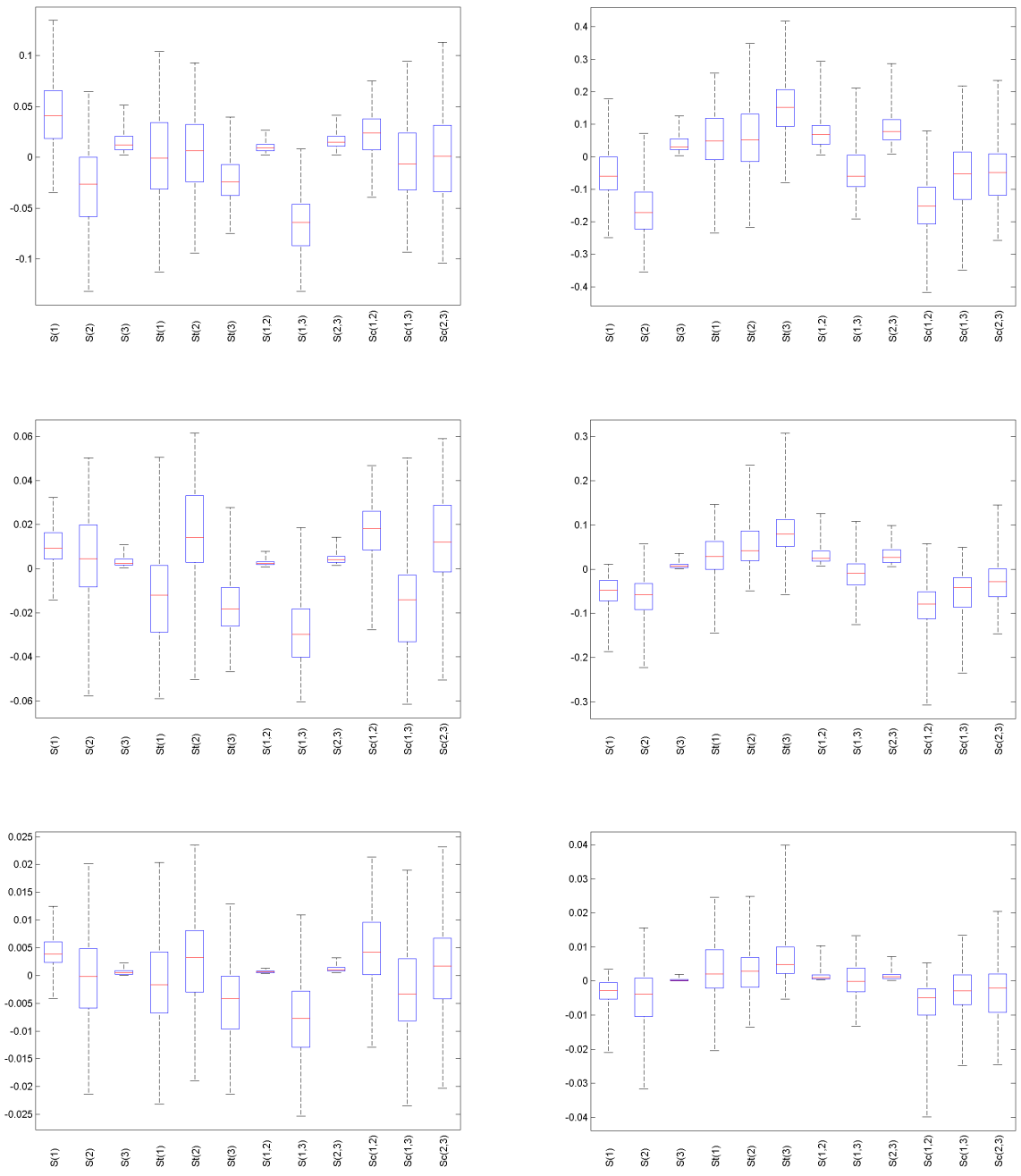

Figure 8: Ishigami function: box-plots of estimation errors of first-order, total, second-order and closed-second-order indices for 100 random Lh designs with $n = 64$ (top), $n = 128$ (middle), $n = 256$ (bottom). Left column: tensorised BLM; right-column: polynomial-chaos model with $D = 5$ (top), $D = 6$, (middle) and $D = 8$ (bottom).

same information as Figure 7, using the same design points. We take $D = 5$, which gives a model with $M = 56$ parameters. We start with a batch of $n_0 = 64$ observations and then estimate $\hat{\boldsymbol{\beta}}^n$ by recursive least-squares, for $n = 65, \ldots, 256$. When the number of observations is small, we are

	S_i	$\overline{S}_i$	$S_{i,j}$	$\underline{S}_{i,j}$
$n = 64$	92	98	100	97
	98	99	67	99
	99	97	100	98
$n = 128$	100	93	99	78
	95	95	59	93
	97	78	96	93
$n = 256$	99	96	99	85
	97	96	73	96
	89	85	65	96

Table 3: Empirical coverage probabilities (in %), for 100 random Lh designs, of approximate 2σ credible intervals for (S_1, S_2, S_3), $(\overline{S}_1, \overline{S}_2, \overline{S}_3)$, $(S_{1,2}, S_{1,3}, S_{2,3})$ and $(\underline{S}_{1,2}, \underline{S}_{1,3}, \underline{S}_{2,3})$ (BLM with $K_{3/2}(x, y; 2)$).

over-confident in the model, although it is not flexible enough to estimate the indices correctly; when n increases, confidence in the model decreases due to a bad fitting with 56 tuning parameters only. Next, using the same random Lh designs as in Figure 8-left, we select the total degree D that gives the best estimation (which is possible here since we know the true value of indices). This gives a model of degree 4 (respectively, 6 and 8), with 35 (respectively, 84 and 165) parameters, when $n = 64$ (respectively, 128 and 256). The results (box-plots) are presented in the right column of Figure 8. Although we have adapted the total degree of the model to the sample size (which is not an easy task in practice), comparison with the left column indicates that performance are significantly worse than with the tensorised BLM.

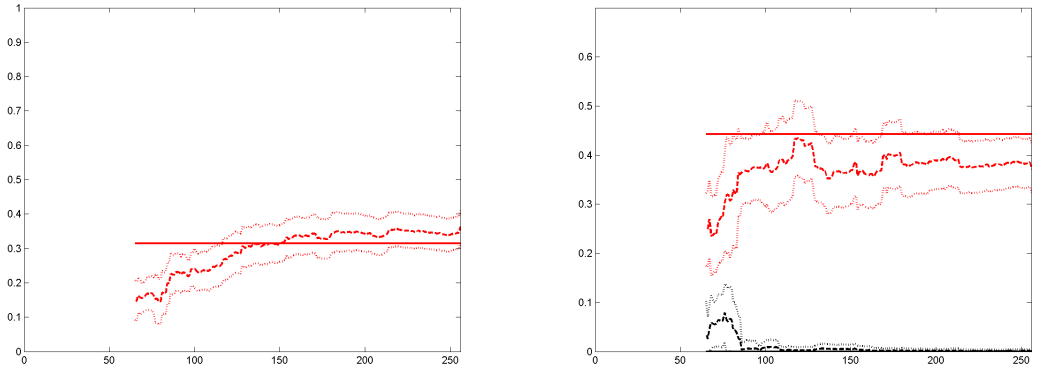

Figure 9: Ishigami function: estimated first-order indices (dashed line) and normal approximation of 95% confidence intervals (dotted lines) with a polynomial-chaos model of total degree $D = 5$; the solid line indicates the true value. Left: S_1; right: S_2 (top) and S_3 (bottom).

Finally; we consider the adaptive designs of Section 6.1. Figure 10 shows the evolution of estimated first order-indices $\widehat{S}_1^n$, like in Figure 7, but when the design points $\mathbf{x}_n$, for $n = 11, \ldots, 256$ are obtained from (6.4) with $\mathscr{X}_Q$ fromed by the first 1,024 points of Sobol' sequence. We observe that convergence to the true values (solid lines) is faster than with the first 256 points of Sobol' sequence used in Figure 7. Figure 11-left shows the evolution of variances (5.6) (used to build the

95% credible intervals in Figure 10); on Figure 11-right the design points $\mathbf{x}_{11}, \ldots, \mathbf{x}_{256}$ are obtained from (6.2).

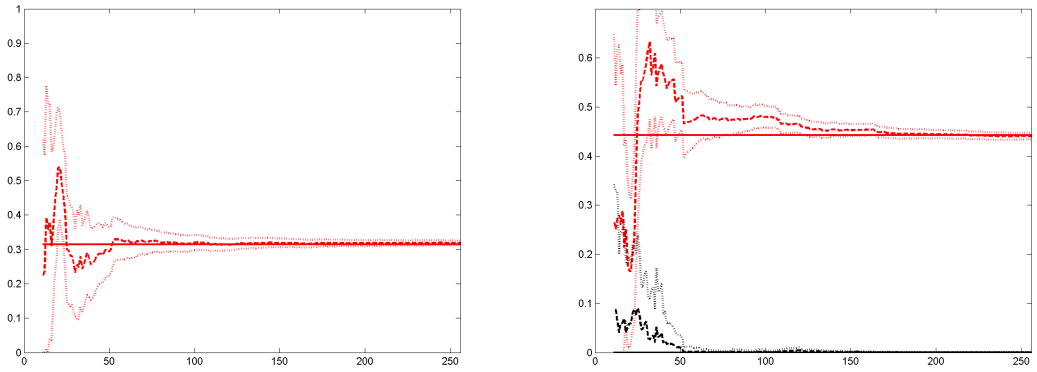

Figure 10: Ishigami function: estimated first-order indices (dashed line) and normal approximation of 95% credible intervals (dotted lines) with a tensorised BLM using $K_{3/2}(x, y; 2)$ and design points given by (6.4); the solid line indicates the true value. Left: S_1; right: S_2 (top) and S_3 (bottom).

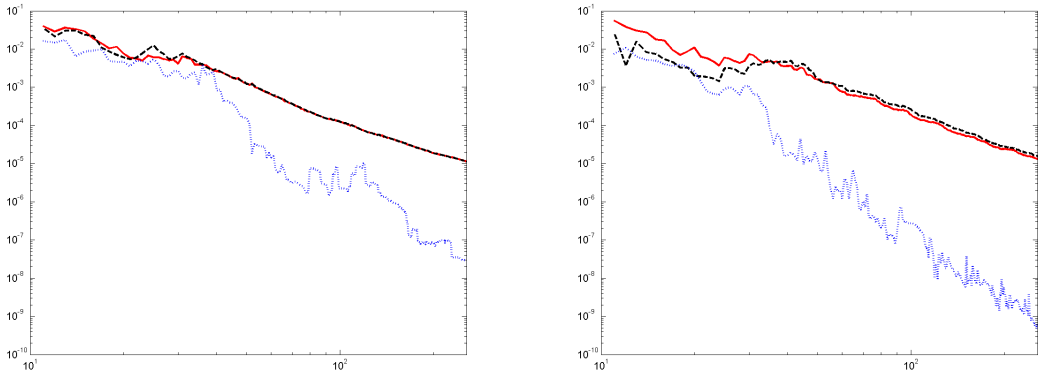

Figure 11: Ishigami function: estimated variances (5.6) of first-order indices S_1 (solid line), S_2 (dashed line) and S_3 (dotted line) as functions of n, for the design sequences (6.4) (left) and (6.2) (right).

7.2 Sobol' g-function

The function is given by $\mathfrak{f}(\mathbf{x}) = \prod_{i=1}^{d} \mathfrak{f}_i(x_i)$ with $\mathfrak{f}_i(x) = (|4x - 2| + a_i)/(a_i + 1)$ for all i and $\mathbf{x}$ uniformly distributed in the unit cube $\mathscr{X} = [0, 1]^d$, the number d of input variables is arbitrary. The index corresponding to any index set $\mathscr{U} = \{i_1, i_2, \ldots, i_s\} \subseteq \{1, \ldots, d\}$ is equal to

$$S_{\mathscr{U}} = \frac{1}{D} \prod_{j=1}^{s} \frac{1}{3} (a_{i_j} + 1)^{-2}$$

where $D = \prod_{i=1}^{d} \left[1 + \frac{1}{3}(a_i + 1)^{-2}\right] - 1$. We use $a_i = i$ in the example. Note that $\mathfrak{f}(\cdot)$ is not differentiable. We take $p_i = 0$ for all i and $K_{3/2}(x, y; 2)$ for the construction of the BLM.

Consider first the case $d = 2$. The design space $\mathscr{X}_Q$ is formed by the first 1,024 points of Sobol' sequence. We take $N = 20$ in (4.5). Figure 12-left shows the adaptive design $\mathbf{x}_{11}, \ldots, \mathbf{x}_{128}$ produced by (6.3) for the estimation of first-order indices S_1 and S_2, when $\mathbf{x}_1, \ldots, \mathbf{x}_{10}$ correspond to the first 10 points of Sobol' sequence. We set $s(\mathbf{x}) = \infty$ after the evaluation of $\mathfrak{f}(\mathbf{x})$ to avoid repetitions, see Remark 6.1. Note that the design obtained is not evenly spread over $\mathscr{X}$ due to the adaptation to the function considered. After the 10 evaluations at $\mathbf{x}_1, \ldots, \mathbf{x}_{10}$ we may also construct a locally optimal design for the next evaluations, using the approach of Section 6.2.2. We substitute $\mathbf{M}_{10}$ for Λ_0^{-1} in (6.8), with $\vartheta = 20$, and take $\mathbf{C} = \mathbf{C}(\hat{\boldsymbol{\beta}}^{10})$ given by (6.5). The optimal design measure, obtained with a vertex-exchange algorithm with $\epsilon = 10^{-5}$, is supported on 20 points. The greedy merging algorithm of Section 6.2.2 (with $\tau = 1.1$ and the selection of an optimal k^* at line 3 based on the comparison between values of $H_\vartheta(\cdot)$), suggests to remove 6 support points. The design obtained is presented on Figure 12-right.

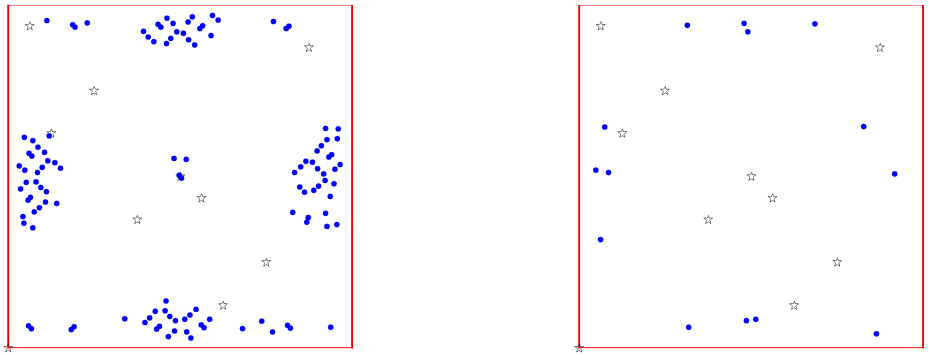

Figure 12: Left: adaptive design (without repetitions, see Remark 6.1) constructed with (6.3) for the estimation of first-order indices in Example 7.2 with $d = 2$ (dots); $n = 128$, the first 10 points (stars) correspond to Sobol' sequence. Right: two-stage design, with the first $n_0 = 10$ points (stars) identical to those on the left part, and the next 14 points (dots) extracted from an optimal measure ξ^* that minimises $\mathrm{trace}[\mathbf{C}(\hat{\boldsymbol{\beta}}^{n_0})\mathbf{M}_\vartheta(\xi)]$, with $\mathbf{M}_{n_0}$ substituted for Λ_0^{-1} in (6.8); ($\vartheta = 20$, $\epsilon = 10^{-5}$, ξ^* is supported on 20 points).

Next, we construct an initial optimal design for the minimisation of the criterion (6.9) with $\vartheta = N = 20$. Note that the construction is independent of the function $\mathfrak{f}(\cdot)$ considered. The ϵ-optimal measure ξ^* ($\epsilon = 10^{-5}$) is now supported on 44 points, and the algorithm of Section 6.2.2 with $\tau = 1.1$ suggests to remove 26 points from ξ^*, see Figure 13-right. The design ξ_{18} extracted is shown on Figure 13-left, where the disk areas are proportional to the weights w_j of ξ_{18}. Similar behaviours are observed in other situations (different values covariance functions for the BLM, different choices for N and ϑ, estimation of different indices, etc.): the designs obtained are typically well spread over $\mathscr{X}$, suggesting that the improvement in terms of the precision of the estimation of indices with respect to a more standard space-filling design is questionable.

Consider finally the case $d = 10$. Figure 14 shows box-plots of the estimation errors $\widehat{S}^n - S$ of first-order and total indices obtained for 100 random Lh designs with $n = 512$ points generated as in Section 7.1. The estimation is much more precise with the BLM model (left) than with polynomial-chaos expansion with total degree $D = 3$ (right) — the model has 286 parameters, the model for $D = 4$ would have 1001 parameters. The true value of the indices are given in Table 4, inspection of Figure 14-left indicates that the estimation of first-order and total indices is already reasonably

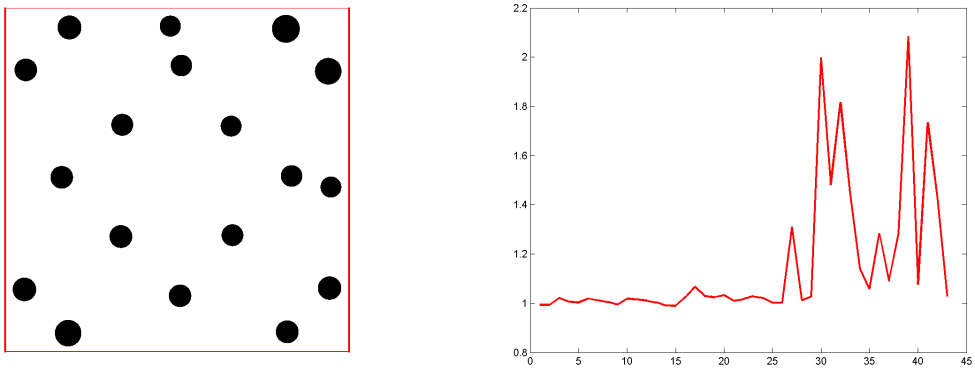

Figure 13: Exact design (18 points) produced by the method of Section 6.2.2 for the estimation of first-order indices in Example 7.2 with $d = 2$ and $\vartheta = N = 20$. Left: design extracted from the ϵ-optimal design measure ξ^* ($\epsilon = 10^{-5}$); ξ^* has 44 support points (not shown), the disk areas are proportional to the weights w_j of ξ_{18}. Right: evolution of ρ_{N^*-k} as a function of k.

accurate for $n = 512$ when using the BLM model (although we only have $\rho(\theta) \simeq 0.6130$ for $\theta = 2$ and all p_i equal to zero, see (4.7), and although $\mathfrak{f}(\cdot)$ is not differentiable). The empirical coverage probabilities, computed as in Section 7.1, are at least 99% for all first-order and total indices.

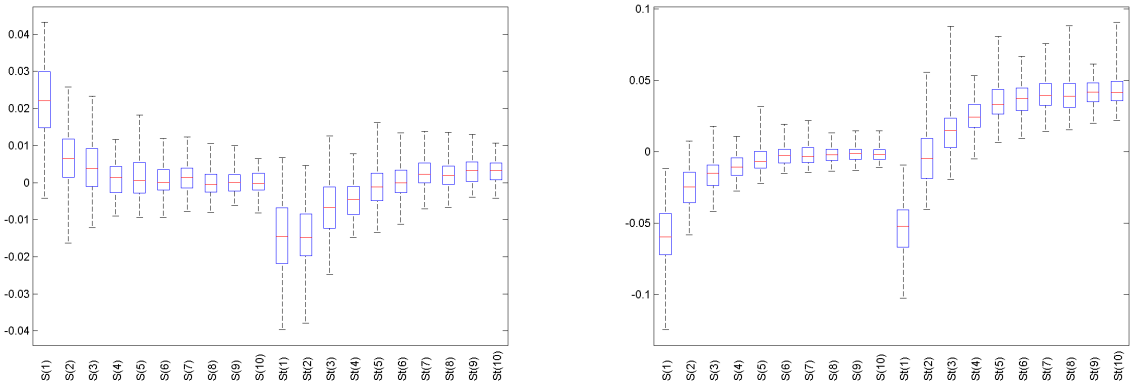

Figure 14: Sobol' g-function for $d = 10$ and $n = 512$: box-plots of estimation errors of first-order and total indices for 100 random Lh designs. Left: tensorised BLM with $K_{3/2}(x, y; 2)$, $\mathrm{p}_i = 0$ for all i and $N = n$ in (4.5); right: polynomial-chaos model with total degree $D = 3$.

8 Conclusions and further developments

A metamodelling approach has been proposed for the estimation of Sobol'indices. It relies on Karhunen-Loéve expansions and combines the flexibility provided by Gaussian-process models with the easy calculations offered by models based on families of orthonormal functions. The computational cost is moderate (it mainly corresponds to the diagonalisation of a few matrices of limited

i	1	2	3	4	5	6	7	8	9	10
S_i	0.4183	0.1859	0.1046	0.0669	0.0465	0.0342	0.0261	0.0207	0.0167	0.0138
$\overline{S}_i$	0.4631	0.2150	0.1229	0.0792	0.0552	0.0407	0.0312	0.0247	0.0200	0.0165

Table 4: First-order and total indices for Sobol' g-function with $d = 10$ and $a_i = i$ for all i.

dimension), and a normal approximation of the posterior distribution of indices is readily available. It can be used to construct experiments adapted to the estimation of Sobol' indices, and various approaches have been considered: sequential, batch sequential, construction of an initial design.

Several points deserve further investigations. The examples shown indicate that the method is efficient for estimating the indices accurately from a moderate number n of function evaluations, but we have not investigated its convergence properties. Consistent estimation can be obtained by letting N (the number of regression functions in the model) and the q_i (number of points in the one-dimensional quadrature approximations) grow fast enough with n, but we do not know the optimal growth rate. Moreover, for fixed n, the choice made in the paper (q_i constant and $N = n$) is surely suboptimal. We observed that the inclusion of orthonormal polynomial terms in the model (i.e., taking $p_i \geq 1$) deteriorates the performance of the method. A general confirmation of this phenomenon would be useful, especially as computations are significantly simpler when all p_i equal zero. We have used a covariance function with a fixed value of the range parameter θ, with a suggestion for choosing θ in agreement with the projected value of n, see (4.7). The estimation of θ based on function evaluations seems a reasonable alternative; see Remark 4.6. It would also be interesting to consider the Bayesian Local Kriging approach of [27], without localisation (i.e., Bayesian Model Averaging [15]), using a (small) set of T different covariance models $K_i^{(t)}(\cdot, \cdot)$, and possibly different polynomial degrees $p_i^{(t)}$, $t = 1, \ldots, T$, for each dimension i. Finally, the construction of optimal experiments adjusted to the estimation of Sobol' indices has been considered in Section 6. Adaptive constructions seem promising, in the sense that they provide (slightly) faster convergence of the estimated indices than more usual low-discrepancy sequences. On the other hand, (initial, off-line) optimal designs exhibit a rather classical space-filling property, and therefore do not seem superior to standard uniform designs.

References

[1] A. Alexanderian. On spectral methods for variance based sensitivity analysis. *Probability Surveys*, 10:51–68, 2013.

[2] G. Blatman and B. Sudret. Efficient computation of global sensitivity indices using sparse polynomial chaos expansions. *Reliability Engineering & System Safety*, 95(11):1216–1229, 2010.

[3] S. Broda and M.S. Paolella. Evaluating the density of ratios of noncentral quadratic forms in normal variables. *Comput. Statist. Data Anal.*, 53:1264–1270, 2009.

[4] E. Burnaev, I. Panin, and B. Sudret. Effective design for Sobol indices estimation based on polynomial chaos expansions. In *Symposium on Conformal and Probabilistic Prediction with Applications*, pages 165–184. Springer, 2016.

[5] R.I. Cukier, C.M. Fortuin, K.E. Shuler, A.G. Petschek, and J.H. Schaibly. Study of the sensi-

tivity of coupled reaction systems to uncertainties in rate coefficients. I Theory. *The Journal of Chemical Physics*, 59(8):3873–3878, 1973.

[6] R.I. Cukier, J.H. Schaibly, and K.E. Shuler. Study of the sensitivity of coupled reaction systems to uncertainties in rate coefficients. III Analysis of the approximations. *The Journal of Chemical Physics*, 63(3):1140–1149, 1975.

[7] N. Durrande, D. Ginsbourger, O. Roustant, and L. Carraro. Anova kernels and RKHS of zero mean functions for model-based sensitivity analysis. *Journal of Multivariate Analysis*, 115:57–67, 2013.

[8] V.V. Fedorov. Design of spatial experiments: model fitting and prediction. In S. Gosh and C.R. Rao, editors, *Handbook of Statistics, vol. 13*, chapter 16, pages 515–553. Elsevier, Amsterdam, 1996.

[9] J.-C. Fort, T. Klein, A. Lagnoux, and B. Laurent. Estimation of the Sobol indices in a linear functional multidimensional model. *Journal of Statistical Planning and Inference*, 143(9):1590–1605, 2013.

[10] B. Gauthier and L. Pronzato. Spectral approximation of the IMSE criterion for optimal designs in kernel-based interpolation models. *SIAM/ASA J. Uncertainty Quantification*, 2:805–825, 2014. DOI 10.1137/130928534.

[11] B. Gauthier and L. Pronzato. Convex relaxation for IMSE optimal design in random field models. *Computational Statistics and Data Analysis*, 113:375–394, 2017.

[12] L. Gilquin, E. Arnaud, C. Prieur, and H. Monod. Recursive estimation procedure of Sobol' indices based on replicated designs. 2016. Preprint hal-01291769.

[13] L. Gilquin, L.A.J. Rugama, E. Arnaud, F.J. Hickernell, H. Monod, and C. Prieur. Iterative construction of replicated designs based on Sobol'sequences. *Comptes Rendus Mathematique*, 355(1):10–14, 2017.

[14] D. Ginsbourger, O. Roustant, D. Schuhmacher, N. Durrande, and N. Lenz. On ANOVA decompositions of kernels and Gaussian random field paths. In *Monte Carlo and Quasi-Monte Carlo Methods*, pages 315–330. Springer, 2016.

[15] J.A. Hoeting, D. Madigan, A.E. Raftery, and C.T. Volinsky. Bayesian model averaging: a tutorial. *Statistical Science*, 14(4):382–417, 1999.

[16] J.P. Imhof. Computing the distribution of quadratic forms in normal variables. *Biometrika*, 48(3 and 4):419–426, 1961.

[17] L. Le Gratiet, C. Cannamela, and B. Iooss. A Bayesian approach for global sensitivity analysis of (multifidelity) computer codes. *SIAM/ASA Journal on Uncertainty Quantification*, 2(1):336–363, 2014.

[18] J. López-Fidalgo, B. Torsney, and R. Ardanuy. MV-optimisation in weighted linear regression. In A.C. Atkinson, L. Pronzato, and H.P. Wynn, editors, *Advances in Model–Oriented Data Analysis and Experimental Design, Proceedings of MODA'5, Marseilles, June 22–26, 1998*, pages 39–50. Physica Verlag, Heidelberg, 1998.

[19] T.A. Mara and O.R. Joseph. Comparison of some efficient methods to evaluate the main effect of computer model factors. *Journal of Statistical Computation and Simulation*, 78(2):167–178, 2008.

[20] A. Marrel, B. Iooss, B. Laurent, and O. Roustant. Calculations of Sobol indices for the Gaussian process metamodel. *Reliability Engineering & System Safety*, 94(3):742–751, 2009.

[21] T.J. Mitchell. An algorithm for the construction of "D-optimal" experimental designs. *Technometrics*, 16:203–210, 1974.

[22] J.E. Oakley and A. O'Hagan. Probabilistic sensitivity analysis of complex models: a Bayesian approach. *Journal of the Royal Statistical Society: Series B (Statistical Methodology)*, 66(3):751–769, 2004.

[23] J. Pilz. *Bayesian Estimation and Experimental Design in Linear Regression Models*, volume 55. Teubner-Texte zur Mathematik, Leipzig, 1983. (also Wiley, New York, 1991).

[24] L. Pronzato. Minimax and maximin space-filling designs: some properties and methods for construction. *Journal de la Société Française de Statistique*, 158(1):7–36, 2017.

[25] L. Pronzato and W.G. Müller. Design of computer experiments: space filling and beyond. *Statistics and Computing*, 22:681–701, 2012.

[26] L. Pronzato and A. Pázman. *Design of Experiments in Nonlinear Models. Asymptotic Normality, Optimality Criteria and Small-Sample Properties.* Springer, LNS 212, New York, 2013.

[27] L. Pronzato and M.-J. Rendas. Bayesian local kriging. *Technometrics*, 2016. to appear, `http://www.tandfonline.com/doi/full/10.1080/00401706.2016.1214179`.

[28] A. Saltelli. Making best use of model evaluations to compute sensitivity indices. *Computer Physics Communications*, 145(2):280–297, 2002.

[29] A. Saltelli, S. Tarantola, and K.P.-S. Chan. A quantitative model-independent method for global sensitivity analysis of model output. *Technometrics*, 41(1):39–56, 1999.

[30] J.H. Schaibly and K.E. Shuler. Study of the sensitivity of coupled reaction systems to uncertainties in rate coefficients. II Applications. *The Journal of Chemical Physics*, 59(8):3879–3888, 1973.

[31] I.M. Sobol'. Sensitivity estimates for nonlinear mathematical models. *Math. Model. Comp. Exp.*, 1(4):407–414, 1993.

[32] M.L. Stein. *Interpolation of Spatial Data. Some Theory for Kriging.* Springer, Heidelberg, 1999.

[33] B. Sudret. Global sensitivity analysis using polynomial chaos expansions. *Reliability Engineering & System Safety*, 93(7):964–979, 2008.

[34] J.-Y. Tissot and C. Prieur. A randomized orthogonal array-based procedure for the estimation of first-and second-order Sobol' indices. *Journal of Statistical Computation and Simulation*, 85(7):1358–1381, 2015.